Partial-wave expansion of the Uehling potential

Peter J. Mohr [*]
National Institute of Standards and Technology, Gaithersburg, Maryland 20899-8420, USA

J. Sapirstein [†]
Department of Physics, University of Notre Dame, Notre Dame, Indiana 46556-5670, USA

(Received 3 April 2023; accepted 15 May 2023; published 7 July 2023)

A coordinate space approach to vacuum polarization using Pauli-Villars regularization is used to calculate the Uehling potential as a partial-wave expansion. This is done to develop a method that can be extended to cases of vacuum polarization where there is no simple analytic form to use to carry out the necessary renormalization. The numerical behavior of the partial-wave expansion is examined for the Uehling potential itself, its contribution to the fine structure of muonic hydrogen, and its contribution to electron scattering.

DOI: 10.1103/PhysRevA.108.012203

I. INTRODUCTION

The ultraviolet divergences of relativistic quantum field theory arise from the short-distance behavior of the products of propagators encountered in loops. An early discussion of how to regulate these divergences was given by Pauli and Villars [1]. Their analysis of vacuum polarization was made in coordinate space, and they used the known short-distance behavior of the propagators to show how a combination of two or more additional terms with a negative metric and large masses $m_1, m_2, \ldots$ could cancel the divergences and give a regularized result.

If one is dealing with free propagators it is convenient to work instead in momentum space, where the propagators have a simple form. However, when studying the effect of vacuum polarization on the energy levels of electrons bound in atoms, the actual propagator differs from a free propagator, and the momentum space representation does not offer a significant advantage. This leads to the general question of how to calculate vacuum polarization for particles whose propagators differ significantly from free propagators, and in particular how to regularize and renormalize in that case.

This is an issue particularly important for highly charged ions, where the strong nuclear Coulomb field leads to so much distortion of the free propagators that both the self-energy and vacuum polarization require an exact treatment. This can be done in coordinate space, where the propagator may be represented as a partial-wave expansion in terms of Whittaker functions. For the case of vacuum polarization, this approach was pioneered by Wichmann and Kroll [2]. They exploited the fact that the calculation with free propagators had already been carried out, with the divergences regularized and the resultant change of the charge dealt with through the renormalization program. Even before the proper treatment of the divergences was carried out, it had been shown that a finite part remained that modified the Coulomb potential of the nucleus. This remainder is known as the Uehling potential and is the largest part of vacuum polarization. As all the ultraviolet divergences were associated with the Uehling potential, Wichmann and Kroll were able to isolate it and thereby evaluate a finite expression as a partial-wave expansion. The so-called Wichmann-Kroll terms require the evaluation of only the first few partial waves even for highly charged ions. One can then add in the Uehling potential, and the treatment of vacuum polarization is complete.

This approach of subtracting the Uehling potential contribution to the vacuum polarization term by term in the angular momentum expansion has been done in many calculations since the Wichmann-Kroll work. For a few examples, see [3–5].

An answer to the general question posed above for atoms might be to work in coordinate space and calculate the difference between the bound-electron propagator and free-electron propagator, with the difference being an ultraviolet-finite expression. One could then separately evaluate the free-electron terms in momentum space and deal with their regularization and renormalization using standard methods. However, the success of this approach relies on the electron propagator at short distances not being qualitatively changed by the presence of a nuclear Coulomb field. If it is necessary to deal with a significantly changed bound-state propagator, the general question is still open. (In the early studies of highly charged ions, the possibility of some breakdown was considered very real.)

In this paper we show that one can calculate atomic vacuum polarization entirely in coordinate space using a partial-wave expansion that includes the Uehling potential. The cost is the need to deal with many partial waves, but the advantage is that one is no longer dependent on using the free-electron propagator to explicitly carry out the renormalization. This approach can be extended to other spherically symmetric central potentials. We formulate the

[*]mohr@nist.gov
[†]jsapirst@nd.edu

renormalization procedure, which is still necessary after the Pauli-Villars regularization, in such a way that it may be applied to the partial-wave expansion without invoking a perturbation expansion to isolate the singularities.

II. FORMALISM

We set up the calculation of vacuum polarization using a representation of the electron propagator intermediate between coordinate and momentum space. Whenever a propagator $S(x_2, x_1)$ depends on the times t_2 and t_1 only through the time difference $\tau \equiv t_2 - t_1$, a Fourier transform allows one to work with a function of two spatial coordinates and one energy parameter, $G(\boldsymbol{x}_2, \boldsymbol{x}_1, z)$, which is the Green function. For electrons it is defined by

$$G(\boldsymbol{x}_2, \boldsymbol{x}_1, z) \equiv -\int d\tau e^{iz\tau/\hbar} S(x_2, x_1)\gamma^0. \tag{1}$$

In the following we work in SI units, keeping all factors of c, $\hbar$, and ϵ_0. The electron and proton charges are denoted q_e and q_p. The elementary charge e is understood to be positive, so $q_e = -e$ and $q_p = e$.

The Green functions are related to the resolvent [6,7], defined formally in terms of a complex number z and an operator A,

$$R(A, z) = \frac{1}{A - z}. \tag{2}$$

If the operator A is taken to be a time-independent Hamiltonian H, the matrix element of the resolvent is $\langle \boldsymbol{x}_2 | R(H, z) | \boldsymbol{x}_1 \rangle = G(\boldsymbol{x}_2, \boldsymbol{x}_1, z)$. A particularly useful form for it comes from inserting complete sets of eigenfunctions ψ_n of H with eigenvalues E_n, which yields

$$G(\boldsymbol{x}_2, \boldsymbol{x}_1, z) = \sum_n \frac{\psi_n(\boldsymbol{x}_2)\psi_n^\dagger(\boldsymbol{x}_1)}{E_n - z}, \tag{3}$$

which is referred to as the spectral decomposition. In Eq. (3) the summation symbol denotes a discrete sum over bound states and integration over the continuous spectrum. The completeness of the eigenfunctions then leads to

$$(H - z)G(\boldsymbol{x}_2, \boldsymbol{x}_1, z) = \delta(\boldsymbol{x}_2 - \boldsymbol{x}_1). \tag{4}$$

Here and in the following, z is understood to be multiplied by a factor of $1 + i\eta$, where η is a positive real infinitesimal, which implements the Feynman contour prescription. The Hamiltonians of interest here can be written in terms of the related Dirac equation,

$$[-i\hbar c\boldsymbol{\alpha} \cdot \boldsymbol{\nabla} + m_e c^2 \beta + V(x) + X(x)\beta]\psi_n(\boldsymbol{x}) = E_n \psi_n(\boldsymbol{x}), \tag{5}$$

with $\boldsymbol{\alpha} = \gamma^0 \boldsymbol{\gamma}$, $\beta = \gamma^0$, and $x = |\boldsymbol{x}|$, and m_e is the electron mass. This class of equations includes several special cases of note. If the functions $V(x)$ and $X(x)$ vanish, we have the free Dirac Hamiltonian and the corresponding Green function, for which we reserve the notation $F(\boldsymbol{x}_2, \boldsymbol{x}_1, z)$. If $X(x)$ vanishes and

$$V(x) = -\frac{\hbar c\alpha}{x} \equiv V_c(x), \tag{6}$$

we have the Coulomb Dirac equation with its corresponding Green function for an electron in a model of the hydrogen atom where the proton is a fixed point charge. The electrostatic potential in this case is

$$\Phi_c(x) = \frac{q_p}{4\pi\epsilon_0 x}, \tag{7}$$

which provides the most studied Green function for the bound-state problem in atomic physics. If we include a factor $Z(x)$,

$$\Phi_Z(x) = \frac{q_p Z(x)}{4\pi\epsilon_0 x}, \tag{8}$$

a number of other useful Green functions can be defined. If $Z(x)$ is chosen as the atomic number Z, one has a starting point for the treatment of hydrogenic ions. If $Z(x)$ is chosen to be a potential that is close to the Hartree-Fock potential (the nonlocality of the latter makes directly using it difficult), one has a lowest-order model for many-electron atoms and ions that can be systematically improved with many-body perturbation theory. If it is chosen to model the charge distribution of a nucleus, one can study finite-size effects on energy levels of those ions. In this case, we have

$$\Phi_{\rm nucl}(x) = \frac{1}{4\pi\epsilon_0} \int d\boldsymbol{x}_1 \frac{q_p\, \rho_{\rm nucl}(x_1)}{|\boldsymbol{x} - \boldsymbol{x}_1|}, \tag{9}$$

where $q_p\, \rho_{\rm nucl}(x_1)$ is the charge distribution of the nucleus, normalized to q_p.

The timelike term $X(x)$ can be used for quark model calculations: in particular, we note the MIT bag model [8] uses such a function to effect confinement. In all cases discussed here, the choice of having the functions depend only on x leads to considerable simplification because one can separate out the angle dependence and carry out the associated integrations analytically.

III. VACUUM POLARIZATION

The one-loop energy level shift due to vacuum polarization for an electron bound to a point charge at the origin with wave function ϕ_n is (see, for example, [9])

$$\Delta E(\rho_n) = \frac{i\alpha\hbar c}{2\pi} \int_{-\infty}^{\infty} dz \int d\boldsymbol{x}_2 \int d\boldsymbol{x}_1 \frac{1}{|\boldsymbol{x}_2 - \boldsymbol{x}_1|} \times \mathrm{Tr}[G(\boldsymbol{x}_2, \boldsymbol{x}_2, z(1 + i\delta))]\rho_n(\boldsymbol{x}_1), \tag{10}$$

where $\rho_n = |\phi_n|^2$. This can be written in terms of the electrostatic potential created by the electron

$$\Phi_n(\boldsymbol{x}_2) = -\frac{e}{4\pi\epsilon_0} \int d\boldsymbol{x}_1 \frac{1}{|\boldsymbol{x}_2 - \boldsymbol{x}_1|} \phi_n^\dagger(\boldsymbol{x}_1)\, \phi_n(\boldsymbol{x}_1) \tag{11}$$

or generalized to the electrostatic potential Φ_ρ associated with an arbitrary charge distribution $e\rho$ given by

$$\Phi_\rho(\boldsymbol{x}_2) = \frac{e}{4\pi\epsilon_0} \int d\boldsymbol{x}_1 \frac{\rho(\boldsymbol{x}_1)}{|\boldsymbol{x}_2 - \boldsymbol{x}_1|}. \tag{12}$$

In this paper we will calculate the change in the interaction energy of a charge density $e\rho_i(\boldsymbol{x})$ in the electrostatic potential $\Phi_c(x)$ of a static point proton at the origin, Eq. (7), caused by the one-loop vacuum polarization for various charge densities. The unperturbed energy is

$$E(\rho) = q_p \Phi_\rho(0), \tag{13}$$

which follows from the relation

$$E(\rho) \equiv e \int d\boldsymbol{x}\, \Phi_{\rm c}(x)\rho(\boldsymbol{x}) = -\epsilon_0 \int d\boldsymbol{x}\, \Phi_{\rm c}(x)\, \nabla^2\, \Phi_\rho(\boldsymbol{x})$$
$$= -\epsilon_0 \int d\boldsymbol{x}\, \Phi_\rho(\boldsymbol{x})\, \nabla^2 \Phi_{\rm c}(x) = q_{\rm p} \int d\boldsymbol{x}\, \Phi_\rho(\boldsymbol{x})\, \delta(\boldsymbol{x}). \tag{14}$$

We will consider three cases. In the first case, the charge density is that of a test charge e at position $\boldsymbol{x}$, $\rho_1(\boldsymbol{x}_2) = e\delta(\boldsymbol{x}_2 - \boldsymbol{x})$. In this case

$$\Phi_1(\boldsymbol{x}_2) = \frac{e}{4\pi\epsilon_0}\frac{1}{|\boldsymbol{x}_2 - \boldsymbol{x}|} \tag{15}$$

and

$$E(\rho_1) = \frac{eq_{\rm p}}{4\pi\epsilon_0 x}. \tag{16}$$

This is just the electrostatic potential of the proton evaluated at the position $\boldsymbol{x}$.

The second charge density is the difference of the charge densities of the $2p$ and $2s$ states of muonic hydrogen, treated nonrelativistically. The potential corresponding to the charge density of the state n is

$$\Phi_n(\boldsymbol{x}_2) = \frac{q_{\rm e}}{4\pi\epsilon_0}\int d\boldsymbol{x}_1\, \frac{|\psi_n(\boldsymbol{x}_1)|^2}{|\boldsymbol{x}_2 - \boldsymbol{x}_1|}, \tag{17}$$

where ψ_n is the Schrödinger wave function. Due to the spherical symmetry of the proton charge distribution, only the spherical average of the electron potential

$$\Phi_n(x_2) = \int \frac{d\Omega_2}{4\pi}\, \Phi_n(\boldsymbol{x}_2)$$
$$= \frac{q_{\rm e}}{4\pi\epsilon_0}\int_0^\infty dx_1\, \frac{x_1^2}{\max(x_2, x_1)} \int d\Omega\, |\psi_n(\boldsymbol{x}_1)|^2 \tag{18}$$

is relevant. The separate potentials are

$$\Phi_{2{\rm p}}(x_2)$$
$$= \frac{q_{\rm e}}{4\pi\epsilon_0 x_2}\left\{1 - \frac{e^{-\gamma x_2}}{24}\left[24 + 18\gamma x_2 + 6(\gamma x_2)^2 + (\gamma x_2)^3\right]\right\}, \tag{19}$$

$$\Phi_{2{\rm s}}(x_2)$$
$$= \frac{q_{\rm e}}{4\pi\epsilon_0 x_2}\left\{1 - \frac{e^{-\gamma x_2}}{8}\left[8 + 6\gamma x_2 + 2(\gamma x_2)^2 + (\gamma x_2)^3\right]\right\}, \tag{20}$$

where $\gamma = \alpha\, m_{\rm r}c/\hbar = \alpha\,(m_{\rm r}/m_{\rm e})/\lambda\!\!\!^{-}_{\rm e}$, where $\lambda\!\!\!^{-}_{\rm e} = \hbar/(m_{\rm e}c)$ is the reduced Compton wavelength of the electron, and $m_{\rm r}$ is the muon reduced mass, with $m_{\rm r}c^2 \approx 95$ MeV. The difference is simply

$$\Phi_2(x_2) = \Phi_{2{\rm p}}(x_2) - \Phi_{2{\rm s}}(x_2) = \frac{q_{\rm e}}{4\pi\epsilon_0 x_2}\,\frac{e^{-\gamma x_2}\,(\gamma x_2)^3}{12} \tag{21}$$

and

$$E(\rho_2) = 0. \tag{22}$$

In the third case, the charge density is of an electron scattering by a static proton with momentum transfer Q, with the potential

$$\Phi_3(\boldsymbol{x}_2) = \frac{q_{\rm e}}{Q^2}\, e^{i\boldsymbol{Q}\cdot\boldsymbol{x}_2/\hbar}, \tag{23}$$

and, rather than an energy,

$$B(\rho_3) = \frac{q_{\rm e}q_{\rm p}}{Q^2} \tag{24}$$

is proportional to the Born amplitude.

The vacuum polarization correction corresponding to any of these charge distributions is

$$\Delta E(\rho)$$
$$= -\frac{ie}{2\pi}\int_{-\infty}^{\infty} dz \int d\boldsymbol{x}_2\, {\rm Tr}[G(\boldsymbol{x}_2, \boldsymbol{x}_2, z(1 + i\eta))\,]\Phi_\rho(\boldsymbol{x}_2).$$
$$= -\frac{ie}{2\pi}\int_{\rm F} dz \int d\boldsymbol{x}_2\, {\rm Tr}[G(\boldsymbol{x}_2, \boldsymbol{x}_2, z)\,]\Phi_\rho(\boldsymbol{x}_2), \tag{25}$$

where F denotes the Feynman contour which passes from $-\infty$ below the negative real z axis, through 0, and to ∞ above the positive real z axis.

We are here interested in the Uehling contribution $\Delta E_{\rm u}$ to the vacuum polarization, which is the linear term in expansion of the Green function in powers of $V_{\rm c}$. The expansion is

$$G(\boldsymbol{x}_2, \boldsymbol{x}_2, z) = F(\boldsymbol{x}_2, \boldsymbol{x}_2, z) + G^{(1)}(\boldsymbol{x}_2, \boldsymbol{x}_2, z) + \cdots, \tag{26}$$

where

$$G^{(1)}(\boldsymbol{x}_2, \boldsymbol{x}_2, z) = -\int d\boldsymbol{x}_1\, F(\boldsymbol{x}_2, \boldsymbol{x}_1, z)V_{\rm c}(x_1)F(\boldsymbol{x}_1, \boldsymbol{x}_2, z), \tag{27}$$

and $F(\boldsymbol{x}_2, \boldsymbol{x}_2, z)$ is the free Green function in Eq. (30). We thus have

$$\Delta E_{\rm u}(\rho) = -\frac{ie}{2\pi}\int_{\rm F} dz \int d\boldsymbol{x}_2\, {\rm Tr}[G^{(1)}(\boldsymbol{x}_2, \boldsymbol{x}_2, z)]\Phi_\rho(\boldsymbol{x}_2)$$
$$= \frac{ie^2}{2\pi}\int_{\rm F} dz \int d\boldsymbol{x}_2 \int d\boldsymbol{x}_1\, \Phi_{\rm c}(x_1)$$
$$\times\, {\rm Tr}[F(\boldsymbol{x}_2, \boldsymbol{x}_1, z)F(\boldsymbol{x}_1, \boldsymbol{x}_2, z)]\Phi_\rho(\boldsymbol{x}_2). \tag{28}$$

An important special case is the free-electron propagator,

$$S_0(x_2, x_1) = \frac{1}{\hbar^4}\int \frac{d^4p}{(2\pi)^4}\,\frac{e^{-i[p_0 c\tau - \boldsymbol{p}\cdot(\boldsymbol{x}_2 - \boldsymbol{x}_1)]/\hbar}}{p_0(1 + i\eta)\gamma^0 - \boldsymbol{\gamma}\cdot\boldsymbol{p} - m_{\rm e}c}. \tag{29}$$

A closed form for the free Green function $F(\boldsymbol{x}_2, \boldsymbol{x}_1, z)$ follows from Eq. (29) as

$$F(\boldsymbol{x}_2, \boldsymbol{x}_1, z) = -\int d\tau e^{iz\tau/\hbar} S_0(x_2, x_1)\gamma^0$$
$$= \frac{1}{\hbar^3}\int \frac{d\boldsymbol{p}}{(2\pi)^3}\,\frac{e^{i\boldsymbol{p}\cdot(\boldsymbol{x}_2 - \boldsymbol{x}_1)/\hbar}}{c\boldsymbol{\alpha}\cdot\boldsymbol{p} + \beta m_{\rm e}c^2 - z}$$
$$= \frac{1}{4\pi(\hbar c)^2}[-i\hbar c\boldsymbol{\alpha}\cdot\boldsymbol{\nabla}_2 + \beta m_{\rm e}c^2 + z]\frac{e^{-c_0|\boldsymbol{x}_2 - \boldsymbol{x}_1|}}{|\boldsymbol{x}_2 - \boldsymbol{x}_1|}$$
$$= \frac{1}{4\pi(\hbar c)^2}\left[i\hbar c\left(c_0 + \frac{1}{|\boldsymbol{x}_2 - \boldsymbol{x}_1|}\right)\frac{\boldsymbol{\alpha}\cdot(\boldsymbol{x}_2 - \boldsymbol{x}_1)}{|\boldsymbol{x}_2 - \boldsymbol{x}_1|}\right.$$
$$\left. + \beta m_{\rm e}c^2 + z\right]\frac{e^{-c_0|\boldsymbol{x}_2 - \boldsymbol{x}_1|}}{|\boldsymbol{x}_2 - \boldsymbol{x}_1|}\quad, \tag{30}$$

where

$$c_0 \equiv \frac{\sqrt{(m_e c^2)^2 - z^2}}{\hbar c}, \quad \mathrm{Re}(c_0) > 0. \tag{31}$$

The function $F(\boldsymbol{x}_2, \boldsymbol{x}_1, z)$ satisfies the equations

$$[-i\hbar c\boldsymbol{\alpha} \cdot \boldsymbol{\nabla}_2 + \beta m_e c^2 - z]F(\boldsymbol{x}_2, \boldsymbol{x}_1, z) = \delta(\boldsymbol{x}_2 - \boldsymbol{x}_1) \tag{32}$$

and

$$F(\boldsymbol{x}_2, \boldsymbol{x}_1, z)[i\hbar c\boldsymbol{\alpha} \cdot \overleftarrow{\boldsymbol{\nabla}}_1 + \beta m_e c^2 - z] = \delta(\boldsymbol{x}_2 - \boldsymbol{x}_1). \tag{33}$$

The latter relation is made evident by the observation that

$$[-i\hbar c\boldsymbol{\alpha} \cdot \boldsymbol{\nabla}_2 + \beta m_e c^2 + z]\frac{e^{-c_0|\boldsymbol{x}_2 - \boldsymbol{x}_1|}}{|\boldsymbol{x}_2 - \boldsymbol{x}_1|} = \frac{e^{-c_0|\boldsymbol{x}_2 - \boldsymbol{x}_1|}}{|\boldsymbol{x}_2 - \boldsymbol{x}_1|}[i\hbar c\boldsymbol{\alpha} \cdot \overleftarrow{\boldsymbol{\nabla}}_1 + \beta m_e c^2 + z] \tag{34}$$

in Eq. (30).

The equations for the vacuum polarization correction given up to this point should be viewed as formal expressions, because it is necessary to modify them to produce nonsingular functions. In particular, it must be noted that each of the terms in Eqs. (26) and (27) is undefined for equal coordinates. However, as shown in [9], if the replacement

$$V_c(x_1) \to V_c(x_1) - V_c(x_2) \tag{35}$$

is made in Eq. (27), then the singularity is canceled in the difference, which vanishes for equal values of the coordinates. Moreover, the integration in Eq. (28) over the subtracted term vanishes when Pauli-Villars regularization is applied to the calculation [9].

On the other hand, Pauli-Villars regularization is sufficient to obtain a finite result for the correction. We begin by reviewing the regularization procedure.

IV. PAULI-VILLARS REGULARIZATION

In order to evaluate Eq. (28), we employ Pauli-Villars (PV) regularization, as mentioned. The basic form of the calculation remains unchanged when this regularization is used, as described in Ref. [9] and chapter 7 of [10]. PV regularization involves the introduction of two regularizing masses m_1 and m_2, taking m_0 to be the electron mass m_e. To cancel the short-distance infinities one introduces the constants

$$C_0 = 1, \quad C_1 = \frac{m_0^2 - m_2^2}{m_2^2 - m_1^2}, \quad C_2 = \frac{m_1^2 - m_0^2}{m_2^2 - m_1^2}, \tag{36}$$

with

$$\sum_{i=0}^{2} C_i = 0, \quad \sum_{i=0}^{2} C_i m_i^2 = 0. \tag{37}$$

We thus redefine $\Delta E_u(\rho)$ to be

$$\Delta E_u(\rho) \equiv -\frac{ie^2}{2\pi}\int_F dz \sum_{i=0}^{2} C_i \int d\boldsymbol{x}_2 \int d\boldsymbol{x}_1 \Phi_c(x_1) \times \mathrm{Tr}[F_i(\boldsymbol{x}_2, \boldsymbol{x}_1, z)F_i(\boldsymbol{x}_1, \boldsymbol{x}_2, z)]\Phi_\rho(\boldsymbol{x}_2), \tag{38}$$

and F_i is the free Green function for a particle with mass m_i. Because the PV method involves several masses we employ the notation $F_i(\boldsymbol{x}_2, \boldsymbol{x}_1, z)$ to denote free Green functions that have the electron mass m_e replaced by m_i and c_0 replaced by $c_i = \sqrt{(m_i c^2)^2 - z^2}/(\hbar c)$, $\mathrm{Re}(c_i) > 0$; the Green function for the electron has subscript $i = 0$ and $m_0 = m_e$.

For the regularized expression, we may rotate the contour of the integral over z to lie along the imaginary z axis. The contributions from the quarter circles at large $|z|$ give no contribution [9]. Thus in terms of the variable u, where $z = iu$, and taking into account the fact that the argument is an even function of u, we have

$$\Delta E_u(\rho) = \frac{e^2}{\pi}\int_0^\infty du \sum_{i=0}^{2} C_i \int d\boldsymbol{x}_2 \int d\boldsymbol{x}_1 \Phi_c(x_1) \times \mathrm{Tr}[F_i(\boldsymbol{x}_2, \boldsymbol{x}_1, iu)F_i(\boldsymbol{x}_1, \boldsymbol{x}_2, iu)]\Phi_\rho(\boldsymbol{x}_2). \tag{39}$$

V. RENORMALIZATION

After regularization, it is necessary to isolate and remove the contribution that corresponds to charge renormalization, which is logarithmically divergent in the limit as the auxiliary masses m_1 and m_2 are taken to infinity. To be explicit, we note that the expression for the vacuum polarization in Eq. (39) can be viewed as the interaction energy between a vacuum polarization electrostatic potential Φ_{vp} and the charge distribution $e\rho$

$$\Delta E_u(\rho) = \int d\boldsymbol{x}\, \Phi_{vp}(\boldsymbol{x})\, e\rho(\boldsymbol{x}), \tag{40}$$

where

$$\Phi_{vp}(\boldsymbol{x}) = \frac{\hbar c\alpha}{\pi}\int_0^\infty du \sum_{i=0}^{2} C_i \int d\boldsymbol{x}_2 \int d\boldsymbol{x}_1 \Phi_c(x_1) \times \mathrm{Tr}[F_i(\boldsymbol{x}_2, \boldsymbol{x}_1, iu)F_i(\boldsymbol{x}_1, \boldsymbol{x}_2, iu)]\frac{1}{|\boldsymbol{x}_2 - \boldsymbol{x}|}. \tag{41}$$

The limiting form of the potential for large $x = |\boldsymbol{x}|$ is taken to be due to a vacuum polarization charge $q_p^{(2)}$ which is defined by

$$\Phi_{vp}(\boldsymbol{x}) \to \frac{1}{4\pi\epsilon_0}\frac{q_p^{(2)}}{x} + \cdots \quad \text{as } x \to \infty \to \frac{\hbar c\alpha}{\pi}\int_0^\infty du \sum_{i=0}^{2} C_i \int d\boldsymbol{x}_2 \int d\boldsymbol{x}_1 \Phi_c(x_1) \times \mathrm{Tr}[F_i(\boldsymbol{x}_2, \boldsymbol{x}_1, iu)F_i(\boldsymbol{x}_1, \boldsymbol{x}_2, iu)]\frac{1}{x} \tag{42}$$

or

$$q_p^{(2)} = \frac{e^2}{\pi}\int_0^\infty du \sum_{i=0}^{2} C_i \int d\boldsymbol{x}_2 \int d\boldsymbol{x}_1 \Phi_c(x_1) \times \mathrm{Tr}[F_i(\boldsymbol{x}_2, \boldsymbol{x}_1, iu)F_i(\boldsymbol{x}_1, \boldsymbol{x}_2, iu)] = \frac{\alpha}{\pi}\frac{q_p}{3}\sum_{i=0}^{2} C_i \ln\left(\frac{m_i}{m_0}\right)^2. \tag{43}$$

See Sec. VI for details.

The charge $q_p^{(2)}$ is infinite in the limit of large regulator masses, so renormalization is invoked as follows. The charge in the zero-order potential in Eq. (7) is taken to be the sum of a

bare charge $q_{\rm p}^{(0)}$ together with the leading vacuum polarization correction,

$$q_{\rm p} = q_{\rm p}^{(0)} + q_{\rm p}^{(2)} + O\big(\alpha\, q_{\rm p}^{(2)}\big), \tag{44}$$

because the observed physical charge is the sum of all contributions. So the potential due to the proton is the sum of the zero-order potential plus the vacuum polarization potential

$$\Phi_{\rm c}^{(0)}(\boldsymbol{x}) + \Phi_{\rm vp}(\boldsymbol{x}) = \frac{q_{\rm p}^{(0)} + q_{\rm p}^{(2)}}{4\pi\epsilon_0|\boldsymbol{x}|} + \widehat{\Phi}_{\rm vp}(\boldsymbol{x}) + O\big(\alpha\, q_{\rm p}^{(2)}\big). \tag{45}$$

The renormalized potential is (see, for example, [9])

$$\begin{aligned}
\widehat{\Phi}_{\rm vp}(\boldsymbol{x}) &= \frac{\hbar c\alpha}{\pi}\int_0^\infty du \sum_{i=0}^{2} C_i \int d\boldsymbol{x}_2 \int d\boldsymbol{x}_1 \Phi_{\rm c}(x_1)\,{\rm Tr}[F_i(\boldsymbol{x}_2,\boldsymbol{x}_1,iu)F_i(\boldsymbol{x}_1,\boldsymbol{x}_2,iu)]\left(\frac{1}{|\boldsymbol{x}_2-\boldsymbol{x}|}-\frac{1}{|\boldsymbol{x}|}\right),\\
&= \frac{\alpha}{3\pi}\,\frac{q_{\rm p}}{4\pi\epsilon_0\, x}\int_1^\infty dt\,\sqrt{t^2-1}\left(\frac{2}{t^2}+\frac{1}{t^4}\right)\sum_{i=0}^{2} C_i\, e^{-2txm_ic/\hbar} \qquad (46)\\
&\to \frac{\alpha}{3\pi}\,\frac{q_{\rm p}}{4\pi\epsilon_0\, x}\int_1^\infty dt\,\sqrt{t^2-1}\left(\frac{2}{t^2}+\frac{1}{t^4}\right) e^{-2txm_{\rm e}c/\hbar}, \qquad (47)
\end{aligned}$$

which is the conventional result for the Uehling potential and is understood to be the limit as $m_1, m_2 \to \infty$. To the order under consideration, the charge $q_{\rm p}$ is the measured charge.

Here we note that this conventional treatment of vacuum polarization is being reviewed in order to show for a known example that the renormaliztion based on the large x limit of the potential may be applied without knowledge of the explicit functional form of the correction, and that it gives the proper result for the Coulomb source charge where explicit expressions are available. It can be expected to be more widely applicable to other cases where the explicit expressions are not necessarily known. In particular, it will be applied term by term to the partial-wave expansion which is the main topic of this study.

VI. ANALYTIC CALCULATION

This section provides an explicit calculation of the vacuum polarization potential in coordinate space. This has been done in Ref. [9], but here it is done without the subtraction introduced in that work to avoid the equal coordinate singularity. Here that singularity is dealt with by the use of PV regularization. This is shown by doing the calculation with the complete, i.e., not expanded in angular momentum, expression for the product of free Green functions. This calculation also provides a check on the numerical code at each step.

The starting point is Eq. (41). It is convenient to parameterize the vacuum polarization potential in terms of a function $T(x)$ through

$$\Phi_{\rm vp}(\boldsymbol{x}) = \frac{\alpha}{\pi}\,\frac{q_{\rm p}}{4\pi\epsilon_0 x}\,T(x), \tag{48}$$

where

$$\begin{aligned}
T(x) = \hbar c\int_0^\infty du \sum_{i=0}^{2} C_i \int d\boldsymbol{x}_2 \int d\boldsymbol{x}_1\,\frac{1}{x_1}\\
\times\,{\rm Tr}[F_i(\boldsymbol{x}_2,\boldsymbol{x}_1,iu)F_i(\boldsymbol{x}_1,\boldsymbol{x}_2,iu)]\frac{x}{\max(x_2,x)}.
\end{aligned} \tag{49}$$

Here we note that the treatment of the formal expression for vacuum polarization requires careful consideration, because the singularities can lead to ambiguities in the result, despite the use of regularization counter-terms. In particular, for the renormalization charge in Eq. (43), if we write [see, for example, Eq. (37) in [9]]

$$\begin{aligned}
&\int d\boldsymbol{x}_2\,{\rm Tr}[F_i(\boldsymbol{x}_2,\boldsymbol{x}_1,z)F_i(\boldsymbol{x}_1,\boldsymbol{x}_2,z)]\\
&= \lim_{\delta\boldsymbol{x}\to 0}\int d\boldsymbol{x}_2\,{\rm Tr}[F_i(\boldsymbol{x}_1,\boldsymbol{x}_2,z)F_i(\boldsymbol{x}_2,\boldsymbol{x}_1-\delta\boldsymbol{x},z)]\\
&= \lim_{\delta\boldsymbol{x}\to 0}\frac{\partial}{\partial z}[F_i(\boldsymbol{x}_1,\boldsymbol{x}_1-\delta\boldsymbol{x},z)] = \lim_{\delta\boldsymbol{x}\to 0}\frac{\partial}{\partial z}\,\frac{z\,e^{-c_i|\delta\boldsymbol{x}|}}{\pi(\hbar c)^2|\delta\boldsymbol{x}|}\\
&= \lim_{\delta\boldsymbol{x}\to 0}\frac{\partial}{\partial z}\,\frac{z}{\pi(\hbar c)^2}\left(\frac{1}{|\delta\boldsymbol{x}|}-c_i+\cdots\right),
\end{aligned} \tag{50}$$

then we have

$$\begin{aligned}
&\int_0^\infty du\sum_{i=0}^{2} C_i\int d\boldsymbol{x}_2\,{\rm Tr}[F_i(\boldsymbol{x}_2,\boldsymbol{x}_1,iu)F_i(\boldsymbol{x}_1,\boldsymbol{x}_2,iu)]\\
&= -\int_0^\infty du\,\frac{\partial}{\partial\, u}\sum_{i=0}^{2} C_i\,\frac{u\,c_i}{\pi(\hbar c)^2}\\
&= -\sum_{i=0}^{2} C_i\,\frac{u\,c_i}{\pi(\hbar c)^2}\bigg|_0^\infty = 0,
\end{aligned} \tag{51}$$

where the surface term at $u=\infty$ vanishes because

$$u\,c_i = \frac{1}{\hbar c}\left[u^2 + \frac{(m_ic^2)^2}{2} - \frac{(m_ic^2)^4}{8u^2}\right] + \cdots, \tag{52}$$

and the leading two terms vanish by the regulator conditions. Although this combination of integrations gives zero, there is still an integral over $\boldsymbol{x}_1$ which yields an infinite result, so the net result is indeterminant. To deal with this, we impose a limit on the radius of the potential due to the charge density ρ,

$$\Phi_\rho(\boldsymbol{x}_2) \to \Phi_\rho(\boldsymbol{x}_2)\,\theta(R-x_2). \tag{53}$$

This removes ambiguities in the calculation, and the effect on the final result may be made arbitrarily small by choosing R to be sufficiently large, but finite.

From Eq. (30), we have

$$\begin{aligned}
&\int d\Omega_2 \int d\Omega_1 \mathrm{Tr}[F_i(\boldsymbol{x}_2, \boldsymbol{x}_1, iu) F_i(\boldsymbol{x}_1, \boldsymbol{x}_2, iu)] \\
&= \frac{2}{(\hbar c)^2} \int_{-1}^{1} d\xi \left[\frac{2c_i}{|\boldsymbol{x}_2 - \boldsymbol{x}_1|} + \frac{1}{|\boldsymbol{x}_2 - \boldsymbol{x}_1|^2} + 2\Big(\frac{m_i c}{\hbar}\Big)^2 \right] \frac{e^{-2c_i|\boldsymbol{x}_2 - \boldsymbol{x}_1|}}{|\boldsymbol{x}_2 - \boldsymbol{x}_1|^2}, \\
&= \frac{1}{(\hbar c)^2} \int_{-1}^{1} d\xi \left[\frac{1}{x_2 x_1} \frac{\partial}{\partial \xi} \left(\frac{2c_i}{|\boldsymbol{x}_2 - \boldsymbol{x}_1|} + \frac{1}{|\boldsymbol{x}_2 - \boldsymbol{x}_1|^2} \right) - \Big(\frac{u}{\hbar c}\Big)^2 \frac{4}{|\boldsymbol{x}_2 - \boldsymbol{x}_1|^2} \right] e^{-2c_i|\boldsymbol{x}_2 - \boldsymbol{x}_1|},
\end{aligned} \tag{54}$$

where ξ is the cosine of the angle between $\boldsymbol{x}_2$ and $\boldsymbol{x}_1$. For the last term, integration by parts over u gives

$$\int_0^\infty du \Big(\frac{u}{\hbar c}\Big)^2 \frac{e^{-2c_i|\boldsymbol{x}_2 - \boldsymbol{x}_1|}}{|\boldsymbol{x}_2 - \boldsymbol{x}_1|^2} = \frac{2}{3} \int_0^\infty du \, \frac{1}{c_i} \Big(\frac{u}{\hbar c}\Big)^4 \frac{e^{-2c_i|\boldsymbol{x}_2 - \boldsymbol{x}_1|}}{|\boldsymbol{x}_2 - \boldsymbol{x}_1|} = \frac{1}{3x_2 x_1} \int_0^\infty du \, \frac{1}{c_i^2} \Big(\frac{u}{\hbar c}\Big)^4 \frac{\partial}{\partial \xi} \, e^{-2c_i|\boldsymbol{x}_2 - \boldsymbol{x}_1|}, \tag{55}$$

and thus

$$\int_0^\infty du \sum_{i=0}^{2} C_i \int d\Omega_2 \int d\Omega_1 \mathrm{Tr}[F_i(\boldsymbol{x}_2, \boldsymbol{x}_1, iu) F_i(\boldsymbol{x}_1, \boldsymbol{x}_2, iu)] = \frac{1}{(\hbar c)^2} \int_0^\infty du \sum_{i=0}^{2} C_i f_i(x_2, x_1, u), \tag{56}$$

where

$$f_i(x_2, x_1, u) = \frac{1}{x_2 x_1} \left\{ \left[\frac{2c_i}{|x_2 - x_1|} + \frac{1}{|x_2 - x_1|^2} - \frac{4}{3c_i^2} \Big(\frac{u}{\hbar c}\Big)^4 \right] e^{-2c_i|x_2 - x_1|} - \left[\frac{2c_i}{x_2 + x_1} + \frac{1}{(x_2 + x_1)^2} - \frac{4}{3c_i^2} \Big(\frac{u}{\hbar c}\Big)^4 \right] e^{-2c_i(x_2 + x_1)} \right\}. \tag{57}$$

To deal with the singularity for $x_2 \approx x_1$, we exclude the interval $(x_2 - \epsilon, x_2 + \epsilon)$ in the integration over x_1 and consider the limit as $\epsilon \to 0$. So we write

$$\begin{aligned}
g_i^{(\epsilon)}(x_2, u) &= \int_0^{x_2 - \epsilon} dx_1 \, x_1 \, f_i(x_2, x_1, u) + \int_{x_2 + \epsilon}^\infty dx_1 \, x_1 \, f_i(x_2, x_1, u) \\
&= \frac{1}{x_2} \left(2 \, \frac{e^{-2c_i\epsilon}}{\epsilon} - 2 \, \frac{e^{-2c_i x_2}}{x_2} + \frac{e^{-2c_i(2x_2 - \epsilon)}}{2x_2 - \epsilon} - \frac{e^{-2c_i(2x_2 + \epsilon)}}{2x_2 + \epsilon} \right) \\
&\quad - \frac{2}{3c_i^3 x_2} \Big(\frac{u}{\hbar c}\Big)^4 (2 \, e^{-2c_i\epsilon} - 2 \, e^{-2c_i x_2} + e^{-2c_i(2x_2 - \epsilon)} - e^{-2c_i(2x_2 + \epsilon)}) \\
&= \frac{1}{x_2} \left(\frac{2}{\epsilon} - 4c_i \right) - 2 \, \frac{e^{-2c_i x_2}}{x_2^2} - \frac{4}{3c_i^3 x_2} \Big(\frac{u}{\hbar c}\Big)^4 (1 - e^{-2c_i x_2}) + O(\epsilon),
\end{aligned} \tag{58}$$

which yields the limit

$$\begin{aligned}
\lim_{\epsilon \to 0} \int_0^\infty du \sum_{i=0}^{2} C_i \, g_i^{(\epsilon)}(x_2, u) &= 2 \int_0^\infty du \sum_{i=0}^{2} C_i \left[\frac{2}{3c_i^3 x_2} \Big(\frac{u}{\hbar c}\Big)^4 - \frac{1}{x_2^2} \right] e^{-2c_i x_2}. \\
&= 4 \int_0^\infty du \sum_{i=0}^{2} C_i \left[\frac{1}{3c_i^3 x_2} \Big(\frac{u}{\hbar c}\Big)^4 - \frac{1}{c_i x_2} \Big(\frac{u}{\hbar c}\Big)^2 \right] e^{-2c_i x_2}.
\end{aligned} \tag{59}$$

The term proportional to $1/\epsilon$ vanishes due to the regulator sum condition, and the integral over u of the second and fourth terms (ignoring parentheses) in the last line of Eq. (58) is zero, because

$$\int_0^\infty du \sum_{i=0}^{2} C_i \left[c_i + \frac{1}{3c_i^3} \Big(\frac{u}{\hbar c}\Big)^4 \right] = \hbar c \int_0^\infty du \sum_{i=0}^{2} C_i \frac{\partial}{\partial u} \left[c_i \Big(\frac{u}{\hbar c}\Big) - \frac{1}{3c_i} \Big(\frac{u}{\hbar c}\Big)^3 \right] = \hbar c \lim_{u \to \infty} \sum_{i=0}^{2} C_i \left[c_i \Big(\frac{u}{\hbar c}\Big) - \frac{1}{3c_i} \Big(\frac{u}{\hbar c}\Big)^3 \right] = 0. \tag{60}$$

Although these terms may be replaced by zero in the analytic calculation if R is finite, they will be present in the numerical calculation, so that errors in the integral over u will be amplified by a factor of order $(R/\lambda\!\!\!^{-}_{\mathrm{e}})^2 \gg 1$. We take this into consideration in the choice of R to be used in the numerical work. We thus have

$$T(x) = \frac{1}{\hbar c} \int_0^\infty du \sum_{i=0}^{2} C_i \left[\frac{1}{3c_i^3} \Big(\frac{u}{\hbar c}\Big)^4 - \frac{1}{c_i} \Big(\frac{u}{\hbar c}\Big)^2 \right] K_i(x, u), \tag{61}$$

where

$$K_i(x,u) = 4\int_0^R dx_2\,\frac{x_2\,x}{\max(x_2,x)}e^{-2c_i x_2}. \tag{62}$$

For the integration over x_2, we consider separately $T(\infty)$ and the renormalized remainder $\widehat{T}(x)$, where

$$\widehat{T}(x) = T(x) - T(\infty). \tag{63}$$

The integrand of the renormalization term $T(\infty)$ is

$$K_i(\infty,u) = 4\int_0^R dx_2\,x_2\,e^{-2c_i x_2} = \frac{1}{c_i^2} + \Delta K_i(\infty,u), \tag{64}$$

which leads to (see Appendix A)

$$T(\infty) = \frac{1}{3}\sum_{i=0}^{2} C_i \ln\left(\frac{m_i}{m_0}\right)^2 + \Delta T(\infty). \tag{65}$$

The extra term $\Delta K_i(\infty,u)$ is

$$\Delta K_i(\infty,u) = -4\int_R^\infty dx_2\,x_2\,e^{-2c_i x_2} = -\frac{1+2c_iR}{c_i^2}\,e^{-2c_iR} \tag{66}$$

and

$$\lim_{R\to\infty}\Delta K_i(\infty,u) = 0. \tag{67}$$

The correction $\Delta T(\infty)$ corresponding to $\Delta K_i(\infty,u)$ can be calculated to find the error that results from using a particular value for R in the numerical calculations.

The renormalized remainder $\widehat{T}(x)$ for $x < R$ follows from

$$\widehat{K}_i(x,u) = 4\int_0^R dx_2\,x_2\left[\frac{x}{\max(x_2,x)} - 1\right]e^{-2c_i x_2} = -\frac{1}{c_i^2}\,e^{-2c_i x} + \Delta\widehat{K}_i(x,u), \tag{68}$$

which gives

$$\widehat{T}(x) = \frac{1}{3}\int_1^\infty dt\,\sqrt{t^2-1}\left(\frac{2}{t^2}+\frac{1}{t^4}\right)\sum_{i=0}^{2} C_i\,e^{-2txm_ic/\hbar} + \Delta\widehat{T}(x) \tag{69}$$

in agreement with Eq. (46). The correction term $\Delta\widehat{T}(x)$ follows from

$$\Delta\widehat{K}_i(x,u) = 4\int_R^\infty dx_2(x_2-x)e^{-2c_i x_2} = \frac{1+2c_i(R-x)}{c_i^2}\,e^{-2c_iR}. \tag{70}$$

VII. PARTIAL WAVE EXPANSION

Having the analytic form of the Green function is of course very useful, but even in cases where such a form is not available, for a spherically symmetric source charge distribution, further progress can be made by expressing the Green function as a partial-wave expansion.

For the free case, the expansion of Eq. (30) is [11]

$$F(\boldsymbol{x}_2,\boldsymbol{x}_1,z) = \frac{c_0}{(\hbar c)^2}\sum_{\kappa\mu}\left[\theta(x_2-x_1)W_\kappa^\mu(\boldsymbol{x}_2,z)U_\kappa^{\mu\dagger}(\boldsymbol{x}_1,z^*) + \theta(x_1-x_2)U_\kappa^\mu(\boldsymbol{x}_2,z)W_\kappa^{\mu\dagger}(\boldsymbol{x}_1,z^*)\right], \tag{71}$$

where $U_\kappa^\mu(\boldsymbol{x},z)$ is regular as $x\to 0$ and $W_\kappa^\mu(\boldsymbol{x},z)$ is regular as $x\to\infty$.

If we define

$$\ell_1 \equiv \left|\kappa+\tfrac{1}{2}\right| - \tfrac{1}{2}, \quad \ell_2 \equiv \left|\kappa-\tfrac{1}{2}\right| - \tfrac{1}{2}, \tag{72}$$

the four-spinor solutions U_κ^μ and W_κ^μ of the free homogeneous Dirac equation with mass m

$$[-i\hbar c\boldsymbol{\alpha}\cdot\boldsymbol{\nabla} + \beta mc^2 - z]U_\kappa^\mu(\boldsymbol{x},z) = 0, \tag{73}$$

$$[-i\hbar c\boldsymbol{\alpha}\cdot\boldsymbol{\nabla} + \beta mc^2 - z]W_\kappa^\mu(\boldsymbol{x},z) = 0 \tag{74}$$

can be written as

$$U_\kappa^\mu(\boldsymbol{x}, z) = \begin{pmatrix} \sqrt{mc^2 + z}\; i_{\ell_1}(c_0 x)\chi_\kappa^\mu(\hat{\boldsymbol{x}}) \\ i\sqrt{mc^2 - z}\; i_{\ell_2}(c_0 x)\chi_{-\kappa}^\mu(\hat{\boldsymbol{x}}) \end{pmatrix} \tag{75}$$

and

$$W_\kappa^\mu(\boldsymbol{x}, z) = \begin{pmatrix} \sqrt{mc^2 + z}\; k_{\ell_1}(c_0 x)\chi_\kappa^\mu(\hat{\boldsymbol{x}}) \\ -i\sqrt{mc^2 - z}\; k_{\ell_2}(c_0 x)\chi_{-\kappa}^\mu(\hat{\boldsymbol{x}}) \end{pmatrix}, \tag{76}$$

where i and k are the modified spherical Bessel functions [12]. The effective adjoints are

$$U_\kappa^{\mu\,\dagger}(\boldsymbol{x}, z^*) = \left(\sqrt{mc^2 + z}\, i_{\ell_1}(c_0 x)\chi_\kappa^{\mu\,\dagger}(\hat{\boldsymbol{x}}) \quad -i\sqrt{mc^2 - z}\, i_{\ell_2}(c_0 x)\chi_{-\kappa}^{\mu\,\dagger}(\hat{\boldsymbol{x}})\right), \tag{77}$$

$$W_\kappa^{\mu\,\dagger}(\boldsymbol{x}, z^*) = \left(\sqrt{mc^2 + z}\, k_{\ell_1}(c_0 x)\chi_\kappa^{\mu\,\dagger}(\hat{\boldsymbol{x}}) \quad i\sqrt{mc^2 - z}\, k_{\ell_2}(c_0 x)\chi_{-\kappa}^{\mu\,\dagger}(\hat{\boldsymbol{x}})\right), \tag{78}$$

and they are solutions of the equations

$$U_\kappa^{\mu\,\dagger}(\boldsymbol{x}, z^*)(i\hbar c\boldsymbol{\alpha} \cdot \overleftarrow{\boldsymbol{\nabla}} + \beta mc^2 - z) = 0, \tag{79}$$

$$W_\kappa^{\mu\,\dagger}(\boldsymbol{x}, z^*)(i\hbar c\boldsymbol{\alpha} \cdot \overleftarrow{\boldsymbol{\nabla}} + \beta mc^2 - z) = 0, \tag{80}$$

corresponding to Eq. (33)

To confirm that the spinors are indeed solutions of the Dirac equation, we employ the identity

$$\boldsymbol{\sigma} \cdot \hat{\boldsymbol{x}}\, \boldsymbol{\sigma} \cdot \boldsymbol{\nabla} = \hat{\boldsymbol{x}} \cdot \boldsymbol{\nabla} + i\, \boldsymbol{\sigma} \cdot (\hat{\boldsymbol{x}} \times \boldsymbol{\nabla}), \quad = \left(\frac{d}{dx} + \frac{1}{x}\right) - \frac{\boldsymbol{\sigma} \cdot \boldsymbol{L} + 1}{x}, \tag{81}$$

and the fact that the Dirac spherical spinors satisfy

$$(\boldsymbol{\sigma} \cdot \boldsymbol{L} + 1)\chi_\kappa^\mu(\hat{\boldsymbol{x}}) = -\kappa\; \chi_\kappa^\mu(\hat{\boldsymbol{x}}), \tag{82}$$

$$\boldsymbol{\sigma} \cdot \hat{\boldsymbol{x}}\; \chi_\kappa^\mu(\hat{\boldsymbol{x}}) = -\chi_{-\kappa}^\mu(\hat{\boldsymbol{x}}), \tag{83}$$

to write

$$\boldsymbol{\sigma} \cdot \boldsymbol{\nabla}\, i_{\ell_1}(c_0 x)\chi_\kappa^\mu(\hat{\boldsymbol{x}}) = -\left(\frac{d}{dx} + \frac{1 + \kappa}{x}\right) i_{\ell_1}(c_0 x)\chi_{-\kappa}^\mu(\hat{\boldsymbol{x}}) = -c_0\, i_{\ell_2}(c_0 x)\chi_{-\kappa}^\mu(\hat{\boldsymbol{x}}), \tag{84}$$

$$\boldsymbol{\sigma} \cdot \boldsymbol{\nabla}\, i_{\ell_2}(c_0 x)\chi_{-\kappa}^\mu(\hat{\boldsymbol{x}}) = -\left(\frac{d}{dx} + \frac{1 - \kappa}{x}\right) i_{\ell_2}(c_0 x)\chi_\kappa^\mu(\hat{\boldsymbol{x}}) = -c_0\, i_{\ell_1}(c_0 x)\chi_\kappa^\mu(\hat{\boldsymbol{x}}), \tag{85}$$

and

$$\boldsymbol{\sigma} \cdot \boldsymbol{\nabla}\, k_{\ell_1}(c_0 x)\chi_\kappa^\mu(\hat{\boldsymbol{x}}) = -\left(\frac{d}{dx} + \frac{1 + \kappa}{x}\right) k_{\ell_1}(c_0 x)\chi_{-\kappa}^\mu(\hat{\boldsymbol{x}}) = c_0\, k_{\ell_2}(c_0 x)\chi_{-\kappa}^\mu(\hat{\boldsymbol{x}}), \tag{86}$$

$$\boldsymbol{\sigma} \cdot \boldsymbol{\nabla}\, k_{\ell_2}(c_0 x)\chi_{-\kappa}^\mu(\hat{\boldsymbol{x}}) = -\left(\frac{d}{dx} + \frac{1 - \kappa}{x}\right) k_{\ell_2}(c_0 x)\chi_\kappa^\mu(\hat{\boldsymbol{x}}) = c_0\, k_{\ell_1}(c_0 x)\chi_\kappa^\mu(\hat{\boldsymbol{x}}). \tag{87}$$

From these relations, Eqs. (73) and (74) can be confirmed. Similarly, taking into account the fact that

$$(c_0 x)^2[i_{\ell_1}(c_0 x)\, k_{\ell_2}(c_0 x) + i_{\ell_2}(c_0 x)\, k_{\ell_1}(c_0 x)] = 1 \tag{88}$$

and the completeness relation

$$\sum_{\kappa\,\mu} \chi_\kappa^\mu(\hat{\boldsymbol{x}}_2)\, \chi_\kappa^{\mu\,\dagger}(\hat{\boldsymbol{x}}_1) = \begin{pmatrix} 1 & 0 \\ 0 & 1 \end{pmatrix} \delta(\phi_2 - \phi_1)\, \delta(\cos\theta_2 - \cos\theta_1), \tag{89}$$

Eq. (71) can be confirmed.

While we will be dealing with here only with the free Green function, when using the partial-wave expansion, other Green functions for spherically symmetric potentials may be expressed similarly, requiring only the replacement of the radial functions. For the Coulomb problem one replaces the spherical Bessel functions by Whittaker functions. If an analytic solution is not available, numerical solutions for the radial function regular at the origin, corresponding to $i_\ell(x)$, or regular at infinity, corresponding to $k_\ell(x)$, can be generated. Thus it is straightforward to extend the method described in this paper to other problems.

VIII. APPLICATION OF THE PARTIAL-WAVE EXPANSION

The central part of this paper, described here, is the coordinate space evaluation of $\Delta E_{\rm u}(\rho)$, given in Eq. (39), using a partial-wave expansion. We can write

$$\Delta E_{\rm u}(\rho) = \frac{e^2}{\pi}\int_0^\infty du \sum_{i=0}^{2} C_i E_i(u,\rho), \tag{90}$$

where

$$E_i(u,\rho) = \int d\boldsymbol{x}_2 \int d\boldsymbol{x}_1 \Phi_{\rm c}(x_1){\rm Tr}[F_i(\boldsymbol{x}_2,\boldsymbol{x}_1,iu)F_i(\boldsymbol{x}_1,\boldsymbol{x}_2,iu)]\Phi_\rho(\boldsymbol{x}_2). \tag{91}$$

The partial-wave expansions of the Green functions entails a breakup into terms that distinguish the relative magnitudes of x_2 and x_1:

$$\begin{aligned} E_i(u,\rho) = {}& \frac{c_i^2}{(\hbar c)^4}\int d\boldsymbol{x}_2 \int d\boldsymbol{x}_1\, \Phi_{\rm c}(x_1)\Phi_\rho(\boldsymbol{x}_2) \\ & \times \sum_{\kappa_1\mu_1}\sum_{\kappa_2\mu_2}\big[\theta(x_2-x_1)W_{\kappa_2}^{\mu_2\,\dagger}(\boldsymbol{x}_2,-iu)W_{\kappa_1}^{\mu_1}(\boldsymbol{x}_2,iu)U_{\kappa_1}^{\mu_1\,\dagger}(\boldsymbol{x}_1,-iu)U_{\kappa_2}^{\mu_2}(\boldsymbol{x}_1,iu) \\ & + \theta(x_1-x_2)U_{\kappa_2}^{\mu_2\,\dagger}(\boldsymbol{x}_2,-iu)U_{\kappa_1}^{\mu_1}(\boldsymbol{x}_2,iu)W_{\kappa_1}^{\mu_1\,\dagger}(\boldsymbol{x}_1,-iu)W_{\kappa_2}^{\mu_2}(\boldsymbol{x}_1,iu)\big]. \end{aligned} \tag{92}$$

The trace allows the matrix reordering to be made, and the integration over Ω_1 forces $\kappa_1=\kappa_2$ and $\mu_1=\mu_2$, which gives

$$\begin{aligned} & \int d\Omega_2 \int d\Omega_1\, \Phi_{\rm c}(x_1)\Phi_\rho(\boldsymbol{x}_2)\, W_{\kappa_2}^{\mu_2\,\dagger}(\boldsymbol{x}_2,-iu)W_{\kappa_1}^{\mu_1}(\boldsymbol{x}_2,iu)U_{\kappa_1}^{\mu_1\,\dagger}(\boldsymbol{x}_1,-iu)U_{\kappa_2}^{\mu_2}(\boldsymbol{x}_1,iu) \\ & = \delta_{\kappa_2\kappa_1}\delta_{\mu_2\mu_1}\Phi_{\rm c}(x_1)\overline{\Phi}_\rho(x_2)\big[(m_ic^2+iu)k_{\ell_1}^2(c_ix_2)+(m_ic^2-iu)k_{\ell_2}^2(c_ix_2)\big] \\ & \quad\times\big[(m_ic^2+iu)i_{\ell_1}^2(c_ix_1)+(m_ic^2-iu)i_{\ell_2}^2(c_ix_1)\big] \end{aligned} \tag{93}$$

and

$$\begin{aligned} & \int d\Omega_2 \int d\Omega_1\, \Phi_{\rm c}(x_1)\Phi_\rho(\boldsymbol{x}_2)\, U_{\kappa_2}^{\mu_2\,\dagger}(\boldsymbol{x}_2,-iu)U_{\kappa_1}^{\mu_1}(\boldsymbol{x}_2,iu)W_{\kappa_1}^{\mu_1\,\dagger}(\boldsymbol{x}_1,-iu)W_{\kappa_2}^{\mu_2}(\boldsymbol{x}_1,iu) \\ & = \delta_{\kappa_2\kappa_1}\delta_{\mu_2\mu_1}\Phi_{\rm c}(x_1)\overline{\Phi}_\rho(x_2)\big[(m_ic^2+iu)i_{\ell_1}^2(c_ix_2)+(m_ic^2-iu)i_{\ell_2}^2(c_ix_2)\big] \\ & \quad\times\big[(m_ic^2+iu)k_{\ell_1}^2(c_ix_1)+(m_ic^2-iu)k_{\ell_2}^2(c_ix_1)\big], \end{aligned} \tag{94}$$

where

$$\overline{\Phi}_\rho(x_2) = \frac{1}{4\pi}\int d\Omega\, \Phi_\rho(\boldsymbol{x}_2), \tag{95}$$

and ℓ_1 and ℓ_2 are defined in Eq. (72) with $\kappa=\kappa_2=\kappa_1$. In the sum over μ_1 and μ_2, one summation remains with no μ dependence, giving a factor $2|\kappa|$.

The integral over u in Eq. (39) includes only positive values of u based on the fact that the argument is an even function of u. This is not the case for the terms in Eqs. (93) and (94) taken individually. However, they are symmetric under the simultaneous change of signs of both κ and u, and the evaluation sums over signs of κ, so the sum is indeed an even function of u.

We thus have

$$\begin{aligned} E_i(u,\rho) = {}& \frac{4}{(\hbar c)^4}c_i^2\int_0^\infty dx_2\, x_2^2\int_0^\infty dx_1\, x_1^2\, \Phi_{\rm c}(x_1)\overline{\Phi}_\rho(x_2)\sum_{|\kappa|=1}^{\infty}|\kappa|\big\{(m^2c^4-u^2)\big[k_{|\kappa|}^2(c_ix_>)i_{|\kappa|}^2(c_ix_<)+k_{|\kappa|-1}^2(c_ix_>)i_{|\kappa|-1}^2(c_ix_<)\big] \\ & +(m^2c^4+u^2)\big[k_{|\kappa|}^2(c_ix_>)i_{|\kappa|-1}^2(c_ix_<)+k_{|\kappa|-1}^2(c_ix_>)i_{|\kappa|}^2(c_ix_<)\big]\big\}, \end{aligned} \tag{96}$$

with $x_< = \min(x_2,x_1)$ and $x_> = \max(x_2,x_1)$.

IX. NUMERICAL ANALYSIS

To carry out the numerical calculation, we form the regularized linear combination of the three values of E_i, choose a value for $|\kappa|$, and carry out the three-dimensional integration. This is also done for a range of partial waves. The calculation could be reordered by first carrying out the partial-wave expansion for a given u, x_2, x_1 until convergence to a given accuracy is achieved, and then doing the integrations: this is can be a more efficient approach but would obscure the purpose of the present paper. Here we are interested in studying the numerical behavior of the partial-wave expansion.

The expression in Eq. (96) can be evaluated with a multidimensional integration package, but modifications are needed in order to deal with numerical instabilities. In this approach, the entire regulated unrenormalized

TABLE I. Values for $T(\infty)$, $\widehat{T}(100\text{ fm})$, and the total $T(100\text{ fm}) = T(\infty) + \widehat{T}(100\text{ fm})$.

Regulator	$T(\infty)$	$\widehat{T}(100\text{ fm})$	$T(100\text{ fm})$	
PV1	−1.320 971	0.309 207	−1.011 764	Eqs. (65) and (69)
PV2	−1.781 447	0.309 854	−1.471 593	
PV3	−2.051 457	0.309 856	−1.741 601	
$m_1, m_2 \to \infty$	$-\infty$	0.309 856	$-\infty$	Eq. (47)

function is calculated and the renormalization is carried out by subtracting the known regulated charge renormalization from the sum over $|\kappa|$. We have done the evaluation this way. In addition, we have done it by repeated one-dimensional Gaussian integrations, where the renormalization is carried out by making the separation discussed in Sec. VI. In this case, the renormalization may be carried out term by term in the partial-wave expansion and prior knowledge of the total charge renormalization is not required. In the general case, the charge renormalization will not be known exactly as it is for the Coulomb field case, so the isolation of the charge renormalization provides a method that may be used for an arbitrary source. Details of this latter approach are given in the following.

Below, the complete functions, not expanded in partial waves, are considered to study their behavior as functions of the regulator masses and the cutoff parameter ϵ.

A. Explicit values for x, the regulator masses, and R

The numerical calculation of the PV regularized function $T(x)$, defined in Eq. (49), is described here. We work with the example $x = 100\text{ fm} = 0.258\,960\,507\,\lambda\!\!\!^{-}_{\rm e}$, and it is necessary to employ particular values for the PV regularization masses discussed in Sec. IV. To do this we choose three pairs of masses, $m_1 = 10\,m_{\rm e}$ and $m_2 = 15\,m_{\rm e}$, which we refer to as the PV1 scheme, $m_1 = 20\,m_{\rm e}$ and $m_2 = 30\,m_{\rm e}$, referred to as the PV2 scheme, and $m_1 = 30\,m_{\rm e}$ and $m_2 = 45\,m_{\rm e}$, for the PV3 scheme. Calculated values for $T(x)$ for the three pairs of values of the regulator masses, broken down into the separate contributions of $T(\infty)$ and $\widehat{T}(100\text{ fm})$, are given in Table I. The value used for the cutoff R, defined in Eq. (53), is $10.0\lambda\!\!\!^{-}_{\rm e}$, which results in truncation errors given by $\Delta T(\infty)$ and $\Delta\widehat{T}(x)$ of 5.5×10^{-10} and -5.4×10^{-10}, respectively. The error values are virtually the same for all three regulator schemes, because the higher-mass counter-terms are negligibly small.

B. The cusp cutoff ϵ

To deal with the singularity for equal coordinates, it is necessary to select a value for the cutoff parameter ϵ as it appears in the integration over x_1 in Eq. (58). If the value is too small, there is roundoff error in the numerical evaluation that would obscure the result. If the value is too large, it will produce a non-negligible change in the value of the integral. To find an acceptable value we calculate the change in the function $h^{(\epsilon)}(x_2)$ as a function of ϵ and x_2, where

$$h^{(\epsilon)}(x_2) = \frac{x_2^2}{\hbar c}\int_0^\infty du \sum_{i=0}^{2} C_i\, g_i^{(\epsilon)}(x_2, u) \tag{97}$$

and

$$\begin{aligned} h(x_2) &= \lim_{\epsilon\to 0} h^{(\epsilon)}(x_2) \\ &= \frac{4}{\hbar c}\int_0^\infty du \sum_{i=0}^{2} C_i\left[\frac{1}{3c_i^3}\left(\frac{u}{\hbar c}\right)^4 - \frac{1}{c_i}\left(\frac{u}{\hbar c}\right)^2\right] x_2\, e^{-2c_i x_2}, \end{aligned} \tag{98}$$

so that

$$T(x) = \int_0^R dx_2\, \frac{x}{\max(x_2, x)}\, h(x_2) + \Delta T(x). \tag{99}$$

Table II lists values of the difference

$$\Delta h(x_2) = h^{(\epsilon)}(x_2) - h(x_2) \tag{100}$$

for various values of ϵ and x_2 for the PVI regulator as an example. The numbers in italics indicate the observed order of magnitude of the roundoff error from the leading term of $1/\epsilon$ in Eq. (58), which would be completely canceled by the regulator subtraction if the numerics were exact. We use quadruple precision in the FORTRAN code, which gives about 32 significant figures. Based on the values in that table, we employ $\epsilon = 10^{-16}\,\lambda\!\!\!^{-}_{\rm e}$ in the calculations, which gives the minimum contribution. For $x_2 \geqslant \lambda\!\!\!^{-}_{\rm e}$, $\Delta h(x_2)$ is essentially independent of x_2, so that

$$\int_0^R dx_2\, \Delta h(x_2) \approx R\Delta h(x_2) \approx 10^{-11} \tag{101}$$

for the working values of R and ϵ. This error would be problematic for $R \to \infty$, and numerical extrapolation to $\epsilon \to 0$ and $R \to \infty$ would yield an ambiguous result.

C. The function $h_{|\kappa|}(x_2)$

The partial-wave expansion of h is given by

$$h(x_2) = \sum_{|\kappa|=1}^{\infty} h_{|\kappa|}(x_2), \tag{102}$$

where

$$\begin{aligned} h_{|\kappa|}(x_2) = \frac{4|\kappa|x_2^2}{(\hbar c)^3}\int_0^\infty du \int_0^\infty dx_1\, x_1 \sum_{i=0}^{2} C_i\, c_i^2 \\ \times \big\{\big(m_i^2c^4 - u^2\big)\big[k_{|\kappa|}^2(c_i x_>) i_{|\kappa|}^2(c_i x_<) \\ + k_{|\kappa|-1}^2(c_i x_>) i_{|\kappa|-1}^2(c_i x_<)\big] \\ + \big(m_i^2c^4 + u^2\big)\big[k_{|\kappa|}^2(c_i x_>) i_{|\kappa|-1}^2(c_i x_<) \\ + k_{|\kappa|-1}^2(c_i x_>) i_{|\kappa|}^2(c_i x_<)\big]\big\}. \end{aligned} \tag{103}$$

TABLE II. The difference $\Delta h(x_2)\lambda\!\!\!^{-}_e$, Eq. (100), as a function of x_2 and ϵ. All values are calculated with the PV1 regulator.

$\epsilon/\lambda\!\!\!^{-}_e$	$x_2 = 0.01\,\lambda\!\!\!^{-}_e$	$x_2 = 0.1\,\lambda\!\!\!^{-}_e$	$x_2 = 1.0\,\lambda\!\!\!^{-}_e$	$x_2 = 10.0\,\lambda\!\!\!^{-}_e$	$x_2 = 100.0\,\lambda\!\!\!^{-}_e$	$x_2 = 1\,000.0\,\lambda\!\!\!^{-}_e$
10^{-6}	2.9×10^{-3}	3.8×10^{-3}	3.7×10^{-3}	3.7×10^{-3}	3.7×10^{-3}	3.7×10^{-3}
10^{-8}	2.9×10^{-5}	3.8×10^{-5}	3.7×10^{-5}	3.7×10^{-5}	3.7×10^{-5}	3.7×10^{-5}
10^{-10}	2.9×10^{-7}	3.8×10^{-7}	3.7×10^{-7}	3.7×10^{-7}	3.7×10^{-7}	3.7×10^{-7}
10^{-12}	2.9×10^{-9}	3.8×10^{-9}	3.7×10^{-9}	3.7×10^{-9}	3.7×10^{-9}	3.7×10^{-9}
10^{-14}	2.9×10^{-11}	3.8×10^{-11}	3.7×10^{-11}	3.7×10^{-11}	3.7×10^{-11}	3.7×10^{-11}
10^{-16}	*10^{-12}*	*10^{-12}*	*10^{-12}*	*10^{-12}*	*10^{-12}*	*10^{-12}*
10^{-18}	*10^{-9}*	*10^{-9}*	*10^{-9}*	*10^{-9}*	*10^{-9}*	*10^{-9}*

The integration over x_1 is carried out as described in Sec. VI, that is, with the replacement

$$\int_0^\infty dx_1 \to \int_0^{x_2-\epsilon} dx_1 + \int_{x_2+\epsilon}^\infty dx_1. \tag{104}$$

Here and in the following, we employ the value $\epsilon = 10^{-16}\,\lambda\!\!\!^{-}_e$ instead of writing or taking the limit. The integrations are done with Gauss-Legendre or Gauss-Laguerre quadrature, as appropriate.

D. Partial sums of $h_{|\kappa|}(x_2)$

We shall ultimately consider the partial-wave expansion of the function $T(x)$, but at this point it is useful to compare partial sums over $|\kappa|$ of $h_{|\kappa|}(x_2)$ to the complete function $h(x_2)$ for two reasons. One is to confirm that the numerical code is correct. The other is to examine the nature of the convergence of the sum, which is one of the goals of this work.

Let

$$H_K(x_2) = \sum_{|\kappa|=1}^{K} h_{|\kappa|}(x_2). \tag{105}$$

Values of these partial sums are listed in Table III.

A few remarks concerning the numbers in Table III may be made. The last row of the table is the exact value of the sum for an infinite number of terms calculated from the analytic result. The extremely small values of $h(x_2)$ for large values of x_2 correspond to the exponential falloff of the complete function. It is evident that there is an extraordinary cancellation among terms within the partial sums to arrive at the value of the complete sum. For $x_2 \leqslant 1.0\,\lambda\!\!\!^{-}_e$, the values are at the limit for $K \geqslant 1\,000$, to the accuracy displayed. At $x_2 = 10.0\,\lambda\!\!\!^{-}_e$, $H_{20\,000}(10.0\,\lambda\!\!\!^{-}_e) = -1.03 \times 10^{-9}/\lambda\!\!\!^{-}_e$, which is consistent with the partial sums approaching the limit. Thus, by construction and numerically in Table III, we have

$$\lim_{K\to\infty} H_K(x_2) = h(x_2). \tag{106}$$

The asymptotic behavior, for large values of x_2, of the function $h_{|\kappa|}(x_2)$ is (see Appendix B)

$$h_{|\kappa|}(x_2) = \frac{4\lambda\!\!\!^{-}_e{}^2|\kappa|}{3x_2^3} \sum_{i=0}^{2} C_i \left(\frac{m_e}{m_i}\right)^2 + \cdots. \tag{107}$$

For the masses in the PV1 regularization scheme, this gives

$$\begin{aligned} h_{|\kappa|}(x_2) &= \frac{2464}{1875}\,\frac{\lambda\!\!\!^{-}_e{}^2\,|\kappa|}{x_2^3} + \cdots \\ &= 1.314\,133\ldots\,\frac{|\kappa|}{\lambda\!\!\!^{-}_e}\left(\frac{\lambda\!\!\!^{-}_e}{x_2}\right)^3 + \cdots. \end{aligned} \tag{108}$$

This limit can be seen in the $K = 1$ row in Table III. The linear growth of the asymptotic value with $|\kappa|$ results in a quadratic growth in the partial sums given by

$$H_K(x_2) = 1.314133\ldots\,\frac{K(K+1)}{2\lambda\!\!\!^{-}_e}\left(\frac{\lambda\!\!\!^{-}_e}{x_2}\right)^3 + \cdots. \tag{109}$$

Values for the examples

$$H_{10}(x_2) = \frac{72.277\ldots}{\lambda\!\!\!^{-}_e}\left(\frac{\lambda\!\!\!^{-}_e}{x_2}\right)^3 + \cdots, \tag{110}$$

$$H_{100}(x_2) = \frac{6636.\ldots}{\lambda\!\!\!^{-}_e}\left(\frac{\lambda\!\!\!^{-}_e}{x_2}\right)^3 \ldots \tag{111}$$

can be seen in the last column of the table. The quadratic growth of the partial sums eventually subsides when the asymptotic condition $|\kappa| \ll x_2/\lambda\!\!\!^{-}_e$ no longer applies. In fact, in Table III the maximum value of each partial sum occurs for $K \approx x_2/\lambda\!\!\!^{-}_e$ and falls off for larger values of K.

TABLE III. Partial sums $H_K(x_2)$ of $h_{|\kappa|}(x_2)$ as defined in Eq. (105) and the complete function $h(x_2)$ given in the last row. All values are calculated with the PV1 regulator and are given in units of $1/\lambda\!\!\!^{-}_e$

K	$x_2 = 0.01\,\lambda\!\!\!^{-}_e$	$x_2 = 0.1\,\lambda\!\!\!^{-}_e$	$x_2 = 1.0\,\lambda\!\!\!^{-}_e$	$x_2 = 10.0\,\lambda\!\!\!^{-}_e$	$x_2 = 100.0\,\lambda\!\!\!^{-}_e$	$x_2 = 1\,000.0\,\lambda\!\!\!^{-}_e$
1	−0.242 598	−2.433 830	0.238 975	$1.319\,611 \times 10^{-3}$	$1.314\,187 \times 10^{-6}$	$1.314\,134 \times 10^{-9}$
10	−0.247 342	−3.277 891	−0.017 383	$3.398\,392 \times 10^{-2}$	$7.149\,646 \times 10^{-5}$	$7.226\,945 \times 10^{-8}$
100	−0.247 343	−3.279 085	−0.224 219	$2.233\,941 \times 10^{-2}$	$3.254\,173 \times 10^{-3}$	$6.569\,073 \times 10^{-6}$
1 000	−0.247 343	−3.279 085	−0.224 359	$1.428\,485 \times 10^{-5}$	$2.250\,145 \times 10^{-3}$	$3.239\,986 \times 10^{-4}$
10 000	−0.247 343	−3.279 085	−0.224 359	$3.550\,016 \times 10^{-10}$	$1.431\,161 \times 10^{-6}$	$2.251\,764 \times 10^{-4}$
∞	−0.247 343	−3.279 085	−0.224 359	$-1.126\,281 \times 10^{-9}$	$-2.445\,408 \times 10^{-88}$	$-1.443\,696 \times 10^{-870}$

TABLE IV. Individual terms $t_{|\kappa|}^{(X)}(\infty)$ and partial sums $T_K^{(X)}(\infty)$ of the incomplete integrals of $h_{|\kappa|}(x_2)$ as defined in Eqs. (116) and (117) with $x = 100$ fm $= 0.258\,960\,507\,\lambda\!\!\!^{-}_{\rm e}$. The last column gives the remainder based on the leading term in the asymptotic expansion for $X = 100\,\lambda\!\!\!^{-}_{\rm e}$. The last row gives values of the incomplete integral over x_2 of the complete sum $T^{(X)}(\infty)$ over $|\kappa|$. All values are calculated with the PV1 regulator.

	$X = 1.0\,\lambda\!\!\!^{-}_{\rm e}$	$X = 10.0\,\lambda\!\!\!^{-}_{\rm e}$	$X = 100.0\,\lambda\!\!\!^{-}_{\rm e}$	$\approx \Delta t_{|\kappa|}^{(X)}(\infty)$
$t_1^{(X)}(\infty)$	−0.312 883	−0.006 584	−0.000 066	0.000 066
$t_2^{(X)}(\infty)$	−0.237 294	−0.012 768	−0.000 131	0.000 131
$t_3^{(X)}(\infty)$	−0.169 218	−0.018 221	−0.000 197	0.000 197
$t_4^{(X)}(\infty)$	−0.122 177	−0.022 759	−0.000 262	0.000 263
$t_5^{(X)}(\infty)$	−0.089 732	−0.026 316	−0.000 328	0.000 329
$T_{10}^{(X)}(\infty)$	−1.137 938	−0.242 772	−0.003 594	0.003 614
$T_{100}^{(X)}(\infty)$	−1.226 549	−1.222 536	−0.227 898	0.331 819
$T_{1000}^{(X)}(\infty)$	−1.226 584	−1.320 935	−1.221 525	32.886 187
$T^{(X)}(\infty)$	−1.226 584	−1.320 971	−1.320 971	

E. Partial wave expansion of the function $T(x)$

To further examine the numerical properties of the partial-wave expansion, we define a function $t_{|\kappa|}^{(X)}(x)$ given by

$$t_{|\kappa|}^{(X)}(x) = \int_0^X dx_2\, \frac{x}{\max(x_2, x)}\, h_{|\kappa|}(x_2), \tag{112}$$

where $X > x$. Partial sums over $|\kappa|$ are denoted by

$$T_K^{(X)}(x) = \sum_{|\kappa|=1}^{K} t_{|\kappa|}^{(X)}(x) = \int_0^X dx_2\, \frac{x}{\max(x_2, x)}\, H_K(x_2). \tag{113}$$

We expect that

$$\lim_{K\to\infty} T_K^{(X)}(x) = T^{(X)}(x) \tag{114}$$

and

$$\lim_{X\to\infty} T^{(X)}(x) = T(x). \tag{115}$$

1. Renormalization term

Following the procedure in Sec. V, we identify the renormalization contributions as

$$t_{|\kappa|}^{(X)}(\infty) = \int_0^X dx_2\, h_{|\kappa|}(x_2) \tag{116}$$

and

$$T_K^{(X)}(x) = \int_0^X dx_2\, H_K(x_2). \tag{117}$$

Calculated values of this function, for several values of X, are given in Table IV. As the table shows, for low angular momenta, the integral over x_2 decreases rapidly as the upper limit X increases. The remainder, the integral from X to ∞,

$$\Delta t_{|\kappa|}^{(X)}(\infty) = \int_X^\infty dx_2\, h_{|\kappa|}(x_2), \tag{118}$$

can be approximated by integration of the asymptotic form of $h_{|\kappa|}(x_2)$ in Eq. (107). This approximation gives

$$\Delta t_{|\kappa|}^{(X)}(\infty) = \frac{2\lambda\!\!\!^{-}_{\rm e}{}^2|\kappa|}{3X^2} \sum_{i=0}^{2} C_i \left(\frac{m_{\rm e}}{m_i}\right)^2 + \cdots. \tag{119}$$

Values of $\Delta t_{|\kappa|}^{(X)}(\infty)$ for $X = 100\,\lambda\!\!\!^{-}_{\rm e}$, based on the leading asymptotic term, are given in the last column in Table IV. The integrals up to $X = 100\,\lambda\!\!\!^{-}_{\rm e}$ plus the estimated remainders, that is, the complete integrals from zero to infinity, appear to be consistent with zero, at least for the lowest values of $|\kappa|$. For higher values of $|\kappa|$, the values in the last column grow rapidly because the leading term of the asymptotic expansion is not a good approximation unless $|\kappa| \ll x_2$.

The fact that these integrals appear to be zero is consistent with the discussion at the start of Sec. VI that suggests such integrals are indeed zero. This raises the interesting question of why the integral of the complete function, that is, the function summed over all values of the angular momentum expansion, is not zero. In fact, these values are listed on the last row of Table IV and they rapidly converge to a nonzero value as the integral is extended to infinity due to the exponential falloff of the integrand for large values of x_2, as shown in Table III.

This seemingly contradictory behavior of the individual terms in the angular momentum expansion and the complete sum can be understood by recalling that the derivation of the complete expression requires a cutoff on the potential, so that an indeterminate product of terms that integrate to zero over the variable u times terms that are infinite when integrated over all space, are finite. This can be seen in Table III, where for a given value of x_2, the partial sums over angular momentum approach the value of the complete expression. Thus with an upper limit on the integration over x_2, the integrals of the partial sums also converge to the integrals over the infinite sums function. On the other hand, for increasing values of x_2 an increasing number of terms in the angular momentum expansion is needed to converge to the value of the complete function.

2. Renormalized remainder

The angular momentum expansion of the renormalized remainder discussed in Sec. VI is based on the terms given by

$$\widehat{t}_{|\kappa|}^{(X)}(x) = t_{|\kappa|}^{(X)}(x) - t_{|\kappa|}^{(X)}(\infty) = \int_x^X dx_2 \left(\frac{x}{x_2} - 1\right) h_{|\kappa|}(x_2), \tag{120}$$

where $X > x$. The corresponding partial sums are

$$\widehat{T}_K^{(X)}(x) = \sum_{|\kappa|=1}^{K} \widehat{t}_{|\kappa|}^{(X)}(x) = \int_x^X dx_2 \left(\frac{x}{x_2} - 1\right) H_K(x_2) \tag{121}$$

and

$$\lim_{K\to\infty} \widehat{T}_K^{(X)}(x) = \widehat{T}^{(X)}(x), \tag{122}$$

$$\lim_{X\to\infty} \widehat{T}^{(X)}(x) = \widehat{T}(x). \tag{123}$$

TABLE V. Individual terms $\widehat{t}^{(X)}_{|\kappa|}(x)$ and partial sums $\widehat{T}^{(X)}_{K}(x)$ of the incomplete integrals of $h_{|\kappa|}(x_2)$ as defined in Eqs. (120) and (121) with $x = 100$ fm $= 0.258\,960\,507\,\lambda\!\!\!^{-}_{\rm e}$. The last column gives the remainder based on the leading term in the asymptotic expansion for $X = 100\,\lambda\!\!\!^{-}_{\rm e}$. The last row gives values of the incomplete integral over x_2 of the complete sum $\widehat{T}^{(X)}(x)$ over $|\kappa|$. All values are calculated with the PV1 regulator.

	$X = 1.0\,\lambda\!\!\!^{-}_{\rm e}$	$X = 10.0\,\lambda\!\!\!^{-}_{\rm e}$	$X = 100.0\,\lambda\!\!\!^{-}_{\rm e}$	$\approx \Delta\widehat{t}^{(X)}_{|\kappa|}(x)$
$\widehat{t}^{(X)}_{1}(x)$	−0.075 605	−0.338 331	−0.344 736	−0.000 066
$\widehat{t}^{(X)}_{2}(x)$	0.022 132	−0.177 353	−0.189 772	−0.000 131
$\widehat{t}^{(X)}_{3}(x)$	0.043 360	−0.094 856	−0.112 571	−0.000 197
$\widehat{t}^{(X)}_{4}(x)$	0.043 772	−0.049 945	−0.072 060	−0.000 262
$\widehat{t}^{(X)}_{5}(x)$	0.038 352	−0.023 566	−0.049 121	−0.000 328
$\widehat{T}^{(X)}_{10}(x)$	0.179 115	−0.643 292	−0.878 610	−0.003 608
$\widehat{T}^{(X)}_{100}(x)$	0.233 036	0.214 692	−0.770 631	−0.331 246
$\widehat{T}^{(X)}_{1000}(x)$	0.233 059	0.309 172	0.210 158	−32.829 412
$\widehat{T}^{(X)}(x)$	0.233 059	0.309 207	0.309 207	

The remainder, the integral from X to ∞,

$$\Delta\widehat{t}^{(X)}_{|\kappa|}(x) = \int_X^\infty dx_2\, h_{|\kappa|}(x_2), \tag{124}$$

is approximated by integration of the asymptotic form in Eq. (107), which gives

$$\Delta\widehat{t}^{(X)}_{|\kappa|}(x) = -\frac{2\lambda\!\!\!^{-}_{\rm e}{}^2|\kappa|}{3X^2}\left(1-\frac{2x}{3X}\right)\sum_{i=0}^{2} C_i\left(\frac{m_{\rm e}}{m_i}\right)^2 + \cdots . \tag{125}$$

Values for the remainder are listed in the last column in Table V. Values of $\widehat{t}^{(X)}_{|\kappa|}(x)$ for $x = 100$ fm and $X = 10.0\,\lambda\!\!\!^{-}_{\rm e}$ are shown in Fig. 1.

F. Muonic hydrogen

The splitting of the $2p_{1/2}$ and $2s_{1/2}$ states in muonic hydrogen is dominated by the Uehling potential, evaluated with

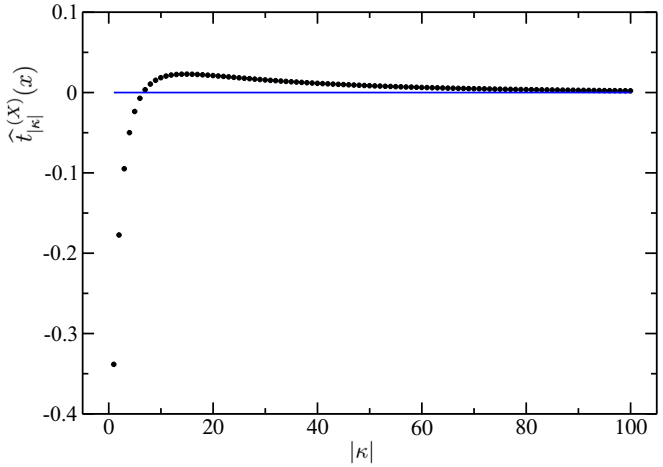

FIG. 1. Values of $\widehat{t}^{(X)}_{|\kappa|}(x)$ for $x = 100$ fm and $X = 10.0\,\lambda\!\!\!^{-}_{\rm e}$

TABLE VI. Values of $\Delta E_{{\rm u},|\kappa|}(\mu{\rm H})$ and the corresponding partial sums $\Delta E^{K}_{\rm u}(\mu{\rm H})$. The last line gives the complete function $\Delta E_{\rm u}(\mu{\rm H})$. All values are in units of meV.

	PV1	PV2	PV3
$\Delta E_{{\rm u},1}(\mu{\rm H})$	−152.758	−177.010	−183.827
$\Delta E_{{\rm u},2}(\mu{\rm H})$	−53.196	−78.387	−86.643
$\Delta E_{{\rm u},3}(\mu{\rm H})$	−8.827	−31.767	−40.343
$\Delta E_{{\rm u},4}(\mu{\rm H})$	10.919	−8.914	−17.302
$\Delta E_{{\rm u},5}(\mu{\rm H})$	19.610	2.955	−4.998
$\Delta E_{{\rm u},6}(\mu{\rm H})$	23.068	9.377	1.977
$\Delta E_{{\rm u},7}(\mu{\rm H})$	23.945	12.905	6.110
$\Delta E_{{\rm u},8}(\mu{\rm H})$	23.527	14.807	8.628
$\Delta E_{{\rm u},9}(\mu{\rm H})$	22.468	15.754	10.178
$\Delta E_{{\rm u},10}(\mu{\rm H})$	21.114	16.119	11.124
$\Delta E^{10}_{\rm u}(\mu{\rm H})$	−70.131	−224.161	−295.096
$\Delta E^{50}_{\rm u}(\mu{\rm H})$	174.495	108.908	32.957
$\Delta E^{100}_{\rm u}(\mu{\rm H})$	193.275	180.231	148.076
$\Delta E^{500}_{\rm u}(\mu{\rm H})$	196.286	202.510	203.382
$\Delta E^{1000}_{\rm u}(\mu{\rm H})$	196.294	202.621	203.879
$\Delta E^{5000}_{\rm u}(\mu{\rm H})$	196.294	202.629	203.919
$\Delta E_{\rm u}(\mu{\rm H})$	196.294	202.629	203.919

nonrelativistic Coulomb wave functions, which contributes 205.007 meV to the theoretical value. The difference between the splitting of 202.3706(23) meV deduced from measurements and the complete theoretical value is used to extract the size of the proton [13]. The one-loop vacuum polarization result is not controversial, but in this section we show how it behaves as a partial-wave expansion.

For this splitting, the difference potential is given in Eq. (21) as

$$\Phi_2(x_2) = \Phi_{2{\rm p}}(x_2) - \Phi_{2{\rm s}}(x_2) = \frac{q_{\rm e}}{4\pi\epsilon_0 x_2}\,\frac{e^{-\gamma x_2}\,(\gamma x_2)^3}{12}.$$

The long-range component of the potentials, given by the leading term in each of Eqs. (19) and (20), would be proportional to the renormalization charge, but they cancel in the difference, so no renormalization is needed for this contribution. However, it is necessary to continue to work with regulated quantities. From Eqs. (7), (21), (90), (96), and (103), we have

$$\Delta E_{\rm u}(\mu{\rm H}) = -\frac{\alpha^2\gamma^3\,\hbar c}{12\pi}\sum_{|\kappa|=1}^{\infty}\int_0^\infty dx_2\, x_2^2\, e^{-\gamma x_2}\, h_{|\kappa|}(x_2). \tag{126}$$

The individual partial-wave contributions are

$$\Delta E_{{\rm u},|\kappa|}(\mu{\rm H}) = -\frac{\alpha^2\gamma^3\,\hbar c}{12\pi}\int_0^\infty dx_2\, x_2^2\, e^{-\gamma x_2}\, h_{|\kappa|}(x_2). \tag{127}$$

In Table VI we list the numerical values of Eq. (127) for the PV1, PV2, and PV3 regulator schemes along with values of partial sums over $|\kappa|$,

$$\Delta E^{K}_{\rm u}(\mu{\rm H}) = \sum_{|\kappa|=1}^{K}\Delta E_{{\rm u},|\kappa|}(\mu{\rm H}), \tag{128}$$

TABLE VII. Values of $\Delta E_{\mathrm{u},|\kappa|}(\mu\mathrm{H})$ for large values of $|\kappa|$ and values of p defined in Eq. (130), all calculated with the PV1 regularization scheme.

$\lvert\kappa\rvert$	$\Delta E_{\mathrm{u},\lvert\kappa\rvert}(\mu\mathrm{H})$	p
100	9.895×10^{-2}	3.94
500	6.293×10^{-5}	4.92
1000	2.031×10^{-6}	4.98
5000	6.569×10^{-10}	5.00

for various upper limits. The partial-wave series starts out with large negative contributions which decrease in magnitude rapidly and change sign to give net positive partial sums, not unlike the behavior shown in Fig. 1. For the PV1 scheme, the positive terms reach a maximum value at $|\kappa| = 7$ and eventually approach zero as $|\kappa|$ increases. As Table VI shows, the partial sums approach the limiting value more slowly for larger values of the regulator masses.

If we assume that the asymptotic form of values of Eq. (127) is given by

$$\Delta E_{\mathrm{u},|\kappa|}(\mu\mathrm{H}) \approx \frac{\text{const}}{|\kappa|^p}, \tag{129}$$

then we can estimate a value for p as

$$p \approx \frac{\ln\left(\frac{\Delta E_{\mathrm{u},|\kappa|}(\mu\mathrm{H})}{\Delta E_{\mathrm{u},|\kappa|+1}(\mu\mathrm{H})}\right)}{\ln\left(\frac{|\kappa|+1}{|\kappa|}\right)}. \tag{130}$$

Table VII gives values of $\Delta E_{\mathrm{u},|\kappa|}(\mu\mathrm{H})$ for large values of $|\kappa|$ and values of p defined in Eq. (130), all calculated with the PV1 regularization scheme. The values for p suggest the asymptotic limit $p \to 5$, although we have not independently confirmed that result.

G. Scattering

The third case we consider is the scattering potential given in Eq. (23). The spherical average is

$$\overline{\Phi}_3(x_2) = \frac{q_\mathrm{e}}{Q^2}\, j_0(Qx_2/\hbar). \tag{131}$$

The corresponding vacuum polarization correction to the Born amplitude is

$$\frac{q_\mathrm{e} q_\mathrm{p}^{(2)}(Q^2)}{Q^2} = \frac{q_\mathrm{e} q_\mathrm{p}}{Q^2}\,\frac{\alpha}{\pi}\,\Pi(Q^2), \tag{132}$$

where (see Sec. IX B)

$$\begin{aligned}\Pi(Q^2) &= \hbar c \int_0^\infty du \sum_{i=0}^{2} C_i \int d\boldsymbol{x}_2 \int d\boldsymbol{x}_1\, \frac{1}{x_1} \\ &\quad \times \mathrm{Tr}[F_i(\boldsymbol{x}_2, \boldsymbol{x}_1, iu) F_i(\boldsymbol{x}_1, \boldsymbol{x}_2, iu)] j_0(Qx_2/\hbar) \\ &= \int_0^\infty dx_2\, j_0(Qx_2/\hbar)\, h(x_2) \\ &= \frac{1}{\hbar c}\int_0^\infty du \sum_{i=0}^{2} C_i \left[\frac{1}{3c_i^3}\left(\frac{u}{\hbar c}\right)^4 - \frac{1}{c_i}\left(\frac{u}{\hbar c}\right)^2\right] \\ &\quad \times \frac{1}{(Q/2\hbar)^2 + c_i^2}\end{aligned} \tag{133}$$

in analogy with Eq. (49). The renormalization constant is

$$\Pi(0) = \frac{1}{3}\sum_{i=0}^{2} C_i \ln\left(\frac{m_i}{m_0}\right)^2, \tag{134}$$

and the renormalized correction factor is

$$\widehat{\Pi}(Q^2) = \Pi(Q^2) - \Pi(0). \tag{135}$$

Note that

$$\Pi(0) = T(\infty), \tag{136}$$

so we do not discuss the renormalization constant any further here.

We reintroduce a cutoff on the potential, as in Eq. (53), to provide a stable numerical evaluation. This can be written as

$$\Pi(Q^2) = \int_0^X dx_2\, j_0(Qx_2/\hbar)\, h(x_2) + \Delta\Pi(Q^2), \tag{137}$$

where

$$\begin{aligned}\Delta\Pi(Q^2) &= \frac{1}{\hbar c}\int_0^\infty du \sum_{i=0}^{2} C_i \left[\frac{1}{3c_i^3}\left(\frac{u}{\hbar c}\right)^4 - \frac{1}{c_i}\left(\frac{u}{\hbar c}\right)^2\right] \\ &\quad \times \frac{e^{-2c_i X}}{(Q/2\hbar)^2 + c_i^2}\left[\cos(QX/\hbar) + \frac{2c_i\hbar}{Q}\sin(QX/\hbar)\right]\end{aligned} \tag{138}$$

and

$$\begin{aligned}\Delta\Pi(0) &= \frac{1}{\hbar c}\int_0^\infty du \sum_{i=0}^{2} C_i \left[\frac{1}{3c_i^3}\left(\frac{u}{\hbar c}\right)^4 - \frac{1}{c_i}\left(\frac{u}{\hbar c}\right)^2\right] \\ &\quad \times \frac{e^{-2c_i X}}{c_i^2}(1 + 2c_i X).\end{aligned} \tag{139}$$

The partial-wave expansion is given by (see Sec. IX C)

$$\widehat{\Pi}_{|\kappa|}(Q^2) = \int_0^X dx_2 [j_0(Qx_2/\hbar) - 1] h_{|\kappa|}(x_2). \tag{140}$$

For the numerical calculation, we consider $Q = 0.1 m_\mathrm{e} c$, with regulator masses $m_1 = 3m_\mathrm{e}$ and $m_2 = 5m_\mathrm{e}$. The cutoff given in Eq. (53) with $R = X$ is included in the evaluation. Table VIII gives the numerical results for various values of the cutoff X, both for the individual terms in Eq. (140) and for the partial sums

$$\widehat{\Pi}^K(Q^2) = \sum_{|\kappa|=1}^{K} \widehat{\Pi}_{|\kappa|}(Q^2). \tag{141}$$

The partial-wave behavior is not much different from that encountered in the previous two cases. In particular, it can be seen that the convergence of the sum over $|\kappa|$ is slower for larger values of the cutoff X. In fact, the convergence appears to be nonuniform, that is, to reach a certain accuracy, the number of terms needed in the partial sum increases as the cutoff X increases.

X. CONCLUSION

We have carried out calculations of vacuum polarization for various applications using a partial-wave expansion in

TABLE VIII. Individual terms $\widehat{\Pi}_{|\kappa|}(Q^2)$ and partial sums over $|\kappa|$, $\widehat{\Pi}^K(Q^2)$, for $Q = 0.1 m_e c$ for various values of the cutoff X in the integration over x_2. The last row gives the complete function $\widehat{\Pi}(Q^2)$.

	$X = 1.0\,\lambda\!\!\!^{-}_e$	$X = 10.0\,\lambda\!\!\!^{-}_e$	$X = 100.0\,\lambda\!\!\!^{-}_e$
$\widehat{\Pi}_1(Q^2)$	0.000 039 219	−0.003 179 729	−0.005 554 317
$\widehat{\Pi}_2(Q^2)$	0.000 072 394	−0.003 665 058	−0.008 305 051
$\widehat{\Pi}_3(Q^2)$	0.000 046 031	−0.003 461 232	−0.010 166 735
$\widehat{\Pi}_4(Q^2)$	0.000 025 263	−0.002 958 788	−0.011 468 983
$\widehat{\Pi}_5(Q^2)$	0.000 013 631	−0.002 354 685	−0.012 379 569
$\widehat{\Pi}^{10}(Q^2)$	0.000 216 333	−0.019 694 567	−0.115 315 317
$\widehat{\Pi}^{100}(Q^2)$	0.000 215 835	0.000 303 838	−0.363 639 445
$\widehat{\Pi}^{1000}(Q^2)$	0.000 215 835	0.000 568 154	−0.001 940 354
$\widehat{\Pi}(Q^2)$	0.000 215 835	0.000 568 188	0.000 568 188

each case. The calculations are (1) the Uehling potential at a given radius in the field of a point charge, (2) the vacuum polarization correction to the Lamb shift in muonic hydrogen, and (3) the vacuum polarization correction to the amplitude for scattering from a point charge. The formalism used is quite general and can be applied to other cases.

An important property of the formulation is the identification of the renormalization charge based on the leading behavior of the unrenormalized vacuum polarization at large distances. This approach does not rely on knowledge of an analytic functional form to calculate the renormalization charge. As a result, the renormalization may be carried out with a term-by-term subtraction in the partial-wave expansion.

The analysis shows that certain details of the calculation require close attention. One issue is the fact that the convergence of the partial wave expansion is seen to depend on the distance from the source charge in a nonuniform manner, with the muonic hydrogen calculation being an exception. This is addressed by introducing a finite cutoff for the range of the potential of the source charge. We have shown that the error due to the cutoff may be made arbitrarily small by making the cutoff sufficiently large. The muonic hydrogen calculation does not require a cutoff, because for the nonrelativistic wavefunctions considered, there is a cancellation between the leading large-distance terms of the potentials of the charge distributions of the S and P states, resulting in an exponentially damped difference potential.

The numerical results also show that the distribution of the partial wave contributions to the total depends on both the regulator masses and the cutoff on the potential of the source charge. Although this may appear to be problematic, the numerics also show that in the limits of large cutoff distance and large regulator masses, the results converge to the values obtained with the conventional approach to the evaluation.

ACKNOWLEDGMENT

J.S. gratefully acknowledges support by the National Institute of Standards and Technology.

APPENDIX A: SINGULAR INTEGRALS

In the vacuum polarization calculation, singular integrals of the form

$$I = \int_0^\infty du \sum_{i=0}^{2} C_i \frac{u^{2n}}{(\hbar c c_i)^{2n+1}}, \quad n = 0, 1, 2, \ldots \tag{A1}$$

occur. Individually, they are logarithmically divergent, but the sum is finite, because the leading asymptotic behavior of the individual integrands is $1/u$, and this vanishes due to the fact that $C_0 + C_1 + C_2 = 0$.

To evaluate the integral, we note that $u^2 = (\hbar c c_i)^2 - (m_i c^2)^2$ to write

$$I = \int_0^\infty du \sum_{i=0}^{2} C_i \frac{u^{2n-2}}{(\hbar c c_i)^{2n-1}} - \int_0^\infty du \sum_{i=0}^{2} C_i \frac{u^{2n-2}(m_i c^2)^2}{(\hbar c c_i)^{2n+1}}. \tag{A2}$$

The second term on the right-hand side vanishes, because there is no dependence on i if the variable change $u \to m_i c^2 u$ is made, and as a consequence, the regulator sum vanishes. This scaling is not possible in Eq. (A1) because the integrals are individually divergent and different scale changes in the integrals cannot simultaneously be made. Evidently, the integrals in Eq. (A1) are independent of n, so we evaluate them all by examining the case $n = 0$.

Starting from

$$\int_0^w du \frac{1}{\hbar c c_i} = \ln\left(\frac{w}{m_i c^2}\right) + \ln\left(1 + \sqrt{1 + \left(\frac{m_i c^2}{w}\right)^2}\right), \tag{A3}$$

we obtain

$$I = \lim_{w\to\infty} \int_0^w du \sum_{i=0}^{2} C_i \frac{1}{\hbar c c_i} = -\frac{1}{2} \sum_{i=0}^{2} C_i \ln\left(\frac{m_i}{m_0}\right)^2. \tag{A4}$$

APPENDIX B: ASYMPTOTIC EXPANSION

This Appendix gives some details of the asymptotic expansion of the function $h_n(x)$ for large x. The asymptotic expansions of the modified spherical Bessel functions are [14]

$$i_n(x) = \frac{e^x}{2x}\left[1 - \frac{n(n+1)}{2x} + \frac{(n-1)n(n+1)(n+2)}{8x^2} + \cdots\right], \tag{B1}$$

$$k_n(x) = \frac{e^{-x}}{x}\left[1 + \frac{n(n+1)}{2x} + \frac{(n-1)n(n+1)(n+2)}{8x^2} + \cdots\right]. \tag{B2}$$

For the function

$$f_{|\kappa|}(m_i, u, x_2, x_1) = |\kappa|\{(m_i^2c^4 - u^2)[k^2_{|\kappa|}(c_ix_>)i^2_{|\kappa|}(c_ix_<) + k^2_{|\kappa|-1}(c_ix_>)i^2_{|\kappa|-1}(c_ix_<)] + (m_i^2c^4 + u^2)[k^2_{|\kappa|}(c_ix_>)i^2_{|\kappa|-1}(c_ix_<) + k^2_{|\kappa|-1}(c_ix_>)i^2_{|\kappa|}(c_ix_<)]\}, \tag{B3}$$

which is implicitly contained in Eq. (103), we define separate terms proportional to m_i^2 and u^2 as

$$f^{(m)}_{|\kappa|}(m_i, u, x_2, x_1) = |\kappa|\, m_i^2c^4[k^2_{|\kappa|}(c_ix_>) + k^2_{|\kappa|-1}(c_ix_>)][i^2_{|\kappa|}(c_ix_<) + i^2_{|\kappa|-1}(c_ix_<)] \tag{B4}$$

and

$$f^{(u)}_{|\kappa|}(m_i, u, x_2, x_1) = -|\kappa|\, u^2[k^2_{|\kappa|}(c_ix_>) - k^2_{|\kappa|-1}(c_ix_>)][i^2_{|\kappa|}(c_ix_<) - i^2_{|\kappa|-1}(c_ix_<)]. \tag{B5}$$

The expansions of the modified spherical Bessel functions yield

$$\int_0^\infty dx_1\, x_1\, f^{(m)}_{|\kappa|}(m_i, u, x_2, x_1) = \frac{|\kappa| m_i^2c^4}{c_i^2(c_ix_2)^2}\left[\frac{1}{c_ix_2} + \frac{1-|\kappa|^2}{2(c_ix_2)^3} + \cdots,\right], \tag{B6}$$

$$\int_0^\infty dx_1\, x_1\, f^{(u)}_{|\kappa|}(m_i, u, x_2, x_1) = \frac{|\kappa|^3u^2}{c_i^2(c_ix_2)^5} + \cdots, \tag{B7}$$

where integration over x_1 is facilitated by making the expansion

$$\frac{1}{x_1} = \frac{1}{x_2} + \frac{x_2 - x_1}{x_2^2} + \frac{(x_2 - x_1)^2}{x_2^3} + \cdots \tag{B8}$$

where necessary. Thus

$$h^{(m)}_{|\kappa|}(x_2) = \frac{4x_2^2}{(\hbar c)^3}\int_0^\infty du \sum_{i=0}^2 C_i\, c_i^2 \int_0^\infty dx_1\, x_1\, f^{(m)}_{|\kappa|}(m_i, u, x_2, x_1) = \frac{4}{3x_2^3}\sum_{i=0}^2 C_i\left(\frac{\hbar}{m_ic}\right)^2 |\kappa|(1-|\kappa|^2) + \cdots, \tag{B9}$$

$$h^{(u)}_{|\kappa|}(x_2) = \frac{4x_2^2}{(\hbar c)^3}\int_0^\infty du \sum_{i=0}^2 C_i\, c_i^2 \int_0^\infty dx_1\, x_1\, f^{(u)}_{|\kappa|}(m_i, u, x_2, x_1) = \frac{4}{3x_2^3}\sum_{i=0}^2 C_i\left(\frac{\hbar}{m_ic}\right)^2 |\kappa|^3 + \cdots, \tag{B10}$$

and

$$h_{|\kappa|}(x_2) = h^{(m)}_{|\kappa|}(x_2) + h^{(u)}_{|\kappa|}(x_2) = \frac{4\lambda\!\!\!^{-}_e{}^2|\kappa|}{3x_2^3}\sum_{i=0}^2 C_i\left(\frac{m_e}{m_i}\right)^2 + \cdots. \tag{B11}$$

For the masses in the PV1 regularization scheme, this gives

$$h_{|\kappa|}(x_2) = \frac{2464}{1875}\frac{\lambda\!\!\!^{-}_e{}^2\,|\kappa|}{x_2^3} + \cdots = 1.314\,133\ldots\frac{\lambda\!\!\!^{-}_e{}^2\,|\kappa|}{x_2^3} + \cdots. \tag{B12}$$

In the limit of large regulator masses, this is just

$$h_{|\kappa|}(x_2) \to \frac{4\lambda\!\!\!^{-}_e{}^2\,|\kappa|}{3x_2^3} = 1.333\,333\ldots\frac{\lambda\!\!\!^{-}_e{}^2\,|\kappa|}{x_2^3}. \tag{B13}$$

[1] W. Pauli and F. Villars, Rev. Mod. Phys. **21**, 434 (1949).
[2] E. H. Wichmann and N. M. Kroll, Phys. Rev. **101**, 843 (1956).
[3] M. Gyulassy, Nucl. Phys. A **244**, 497 (1975).
[4] G. Soff and P. J. Mohr, Phys. Rev. A **38**, 5066 (1988).
[5] H. Persson, I. Lindgren, S. Salomonson, and P. Sunnergren, Phys. Rev. A **48**, 2772 (1993).
[6] A. Messiah, *Quantum Mechanics* (John Wiley and Sons, New York, 1963), p. 712.
[7] B. Friedman, *Principles and Techniques of Applied Mathematics* (John Wiley and Sons, New York, 1956).
[8] A. Chodos, R. L. Jaffe, K. Johnson, C. B. Thorn, and V. F. Weisskopf, Phys. Rev. D **9**, 3471 (1974).
[9] P. Indelicato, P. J. Mohr, and J. Sapirstein, Phys. Rev. A **89**, 042121 (2014).
[10] C. Itzykson and J.-B. Zuber, *Quantum Field Theory* (Dover Publications, Mineola, NY, 1980), p. 318.
[11] P. J. Mohr, G. Plunien, and G. Soff, Phys. Rep. **293**, 227 (1998).
[12] G. B. Arfken, H. J. Weber, and F. E. Harris, *Methematical Methods for Physicists* (Elsevier, Amsterdam, 2013).
[13] A. Antognini *et al.*, Science **339**, 417 (2013).
[14] NIST digital library of mathematical functions, release 1.1.5, http://dlmf.nist.gov (2022).